



CSST双星科学研究所

课题参与人员：

陈雪飞、韩占文、吕国梁、陈海亮、赵景昆、李荫碧

张孝斌、余聪、张泳、任娟娟、聂俊丹、徐晓杰、罗杨平、罗常青、张先飞、田志佳、李蛟、章博、李江丹

特别感谢：刘超、季凯帆

参与研究的研究生：李佳佳、饶加睿、谢薇、周曾华、郭彦君、李江丹

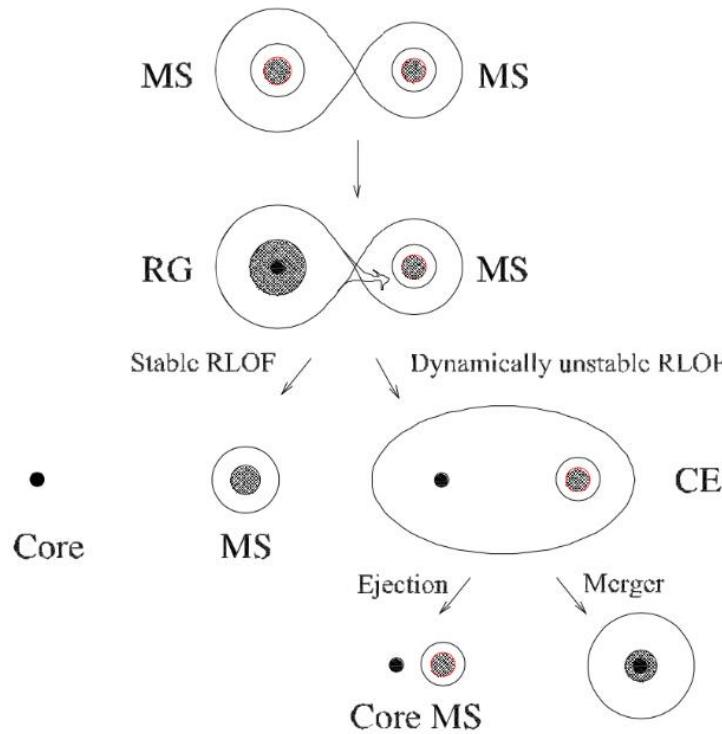
2022-09-28

提 纲

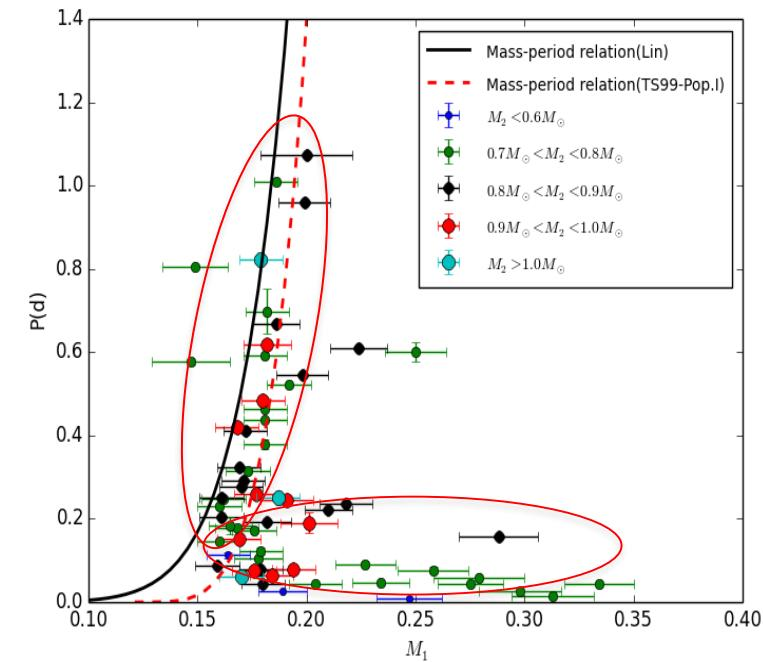
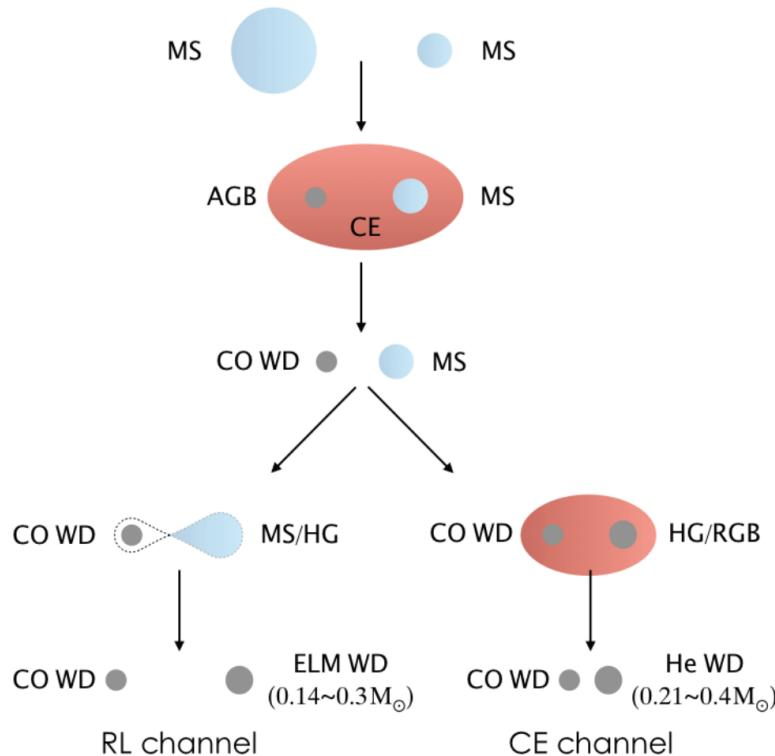
- 双星演化的背景和意义
- CSST双星课题的设置
- 研究进展

Basic Processes in Binary Evolution

~ 50 % stars are in binaries

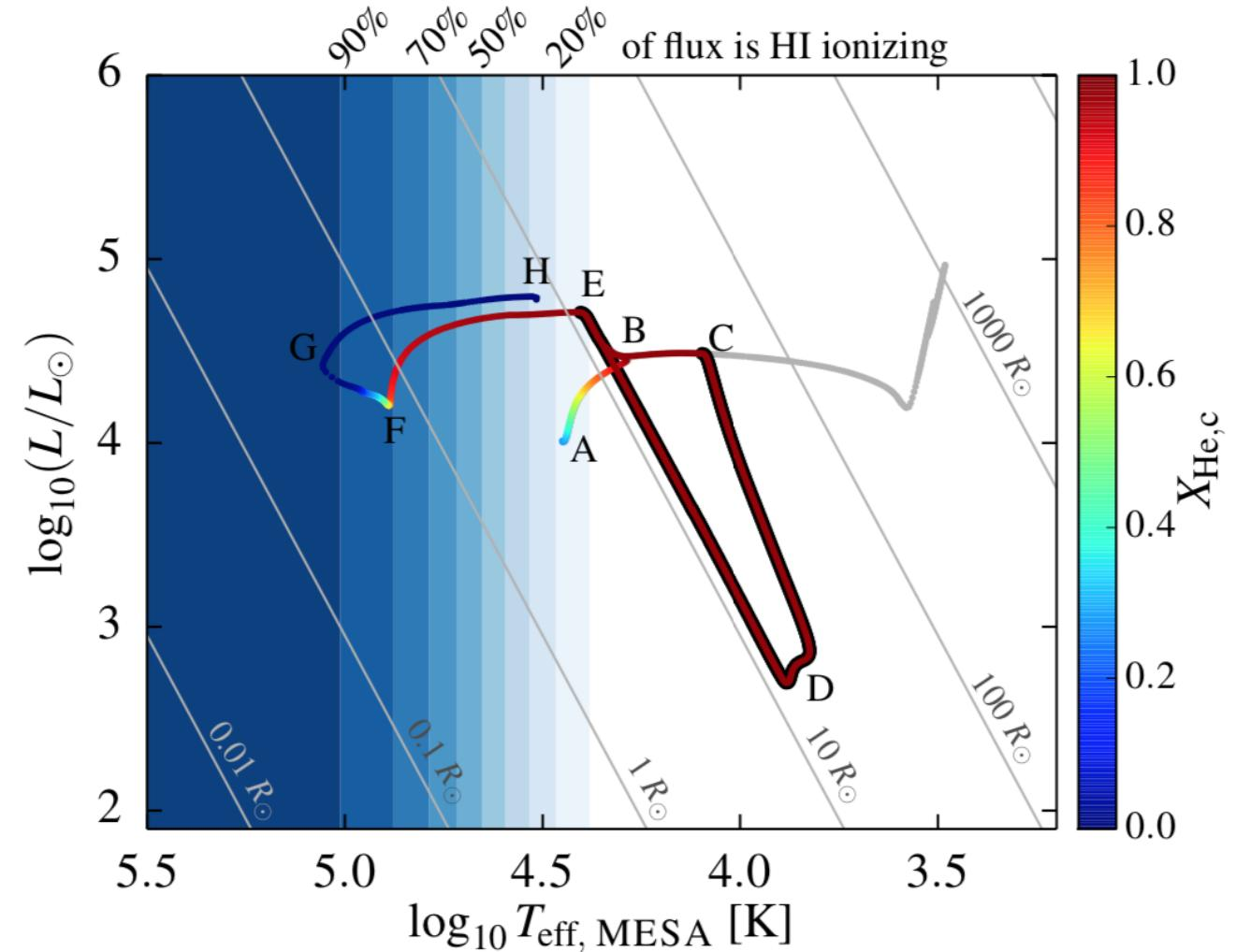
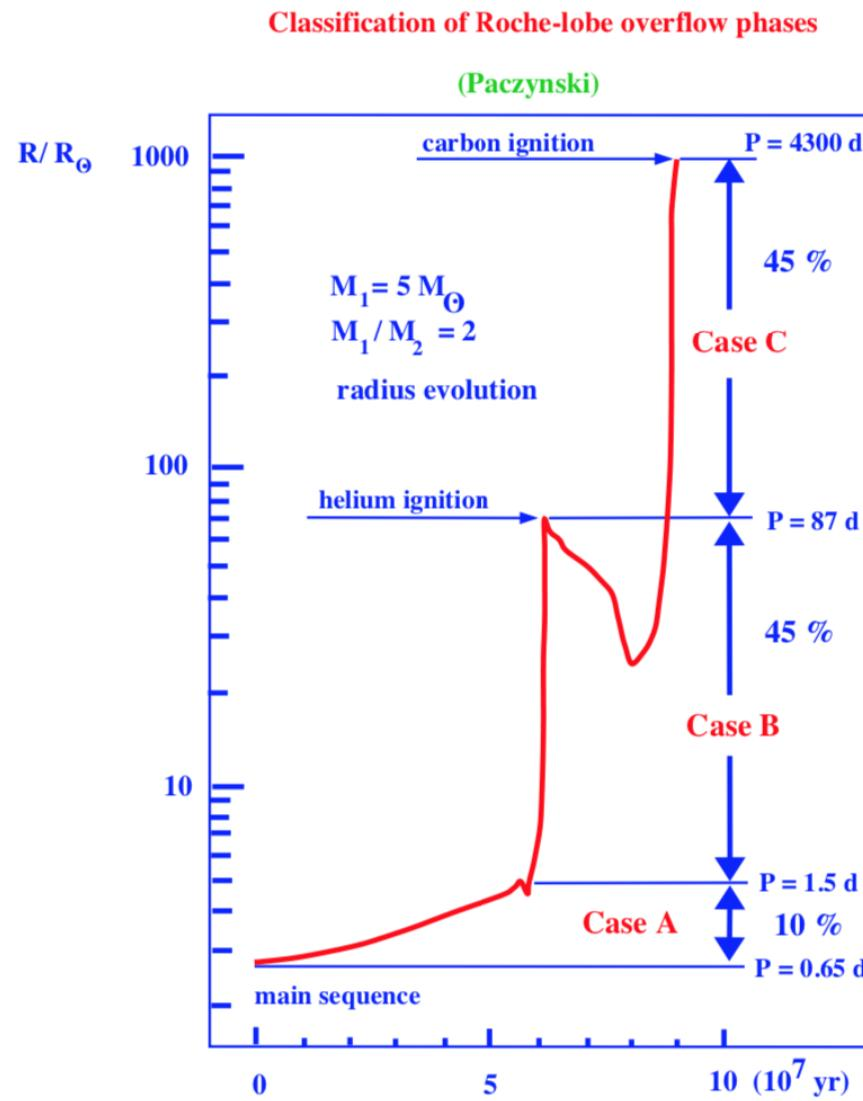


Double white dwarfs with extremely low-mass WDs



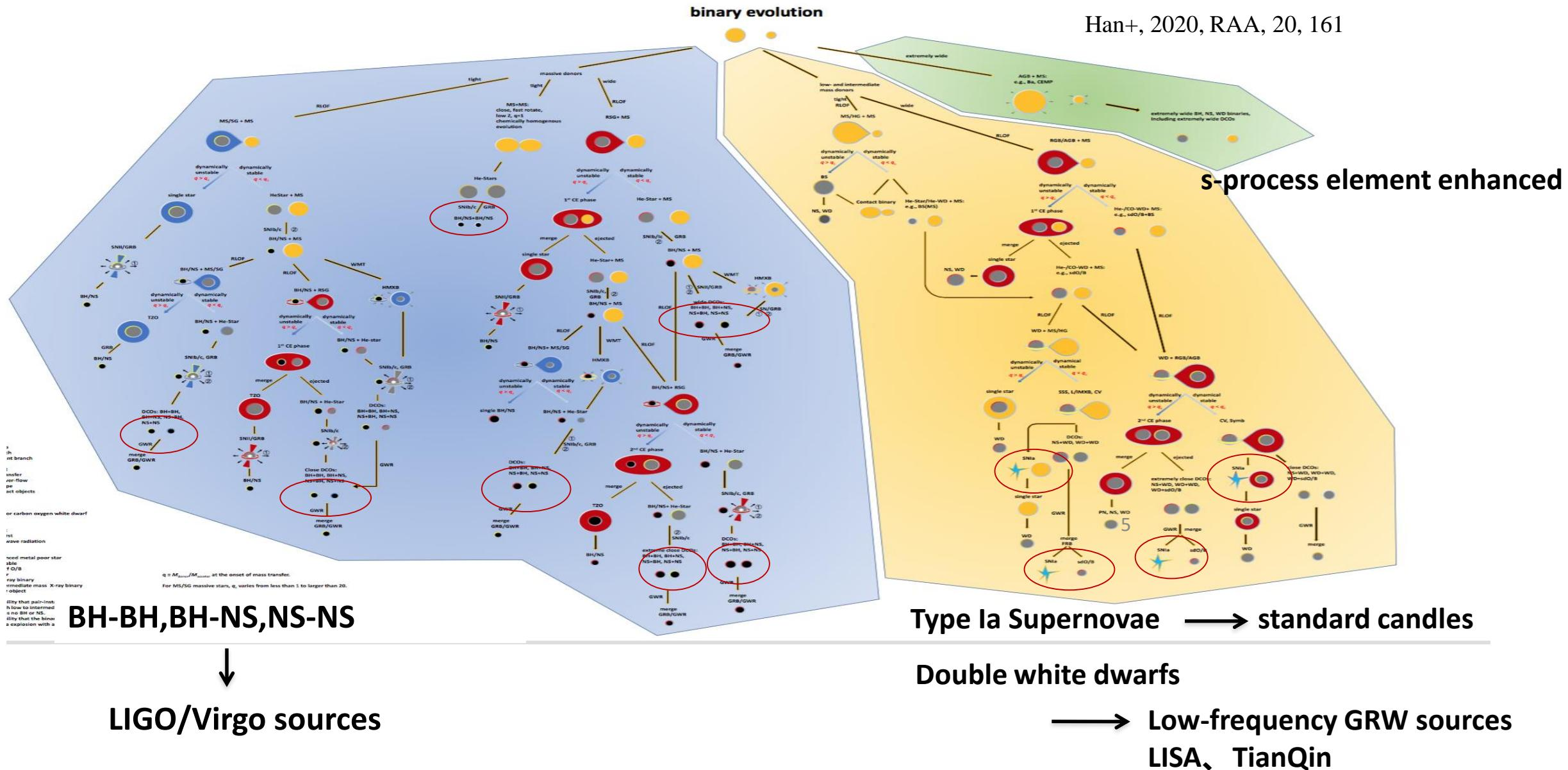
Li+, 2019, ApJ

Binary evolution – changes destiny of stars



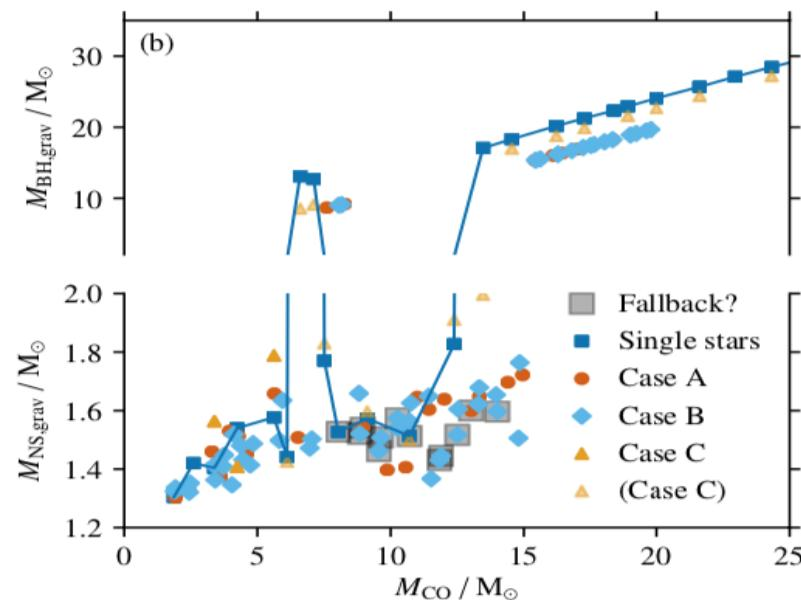
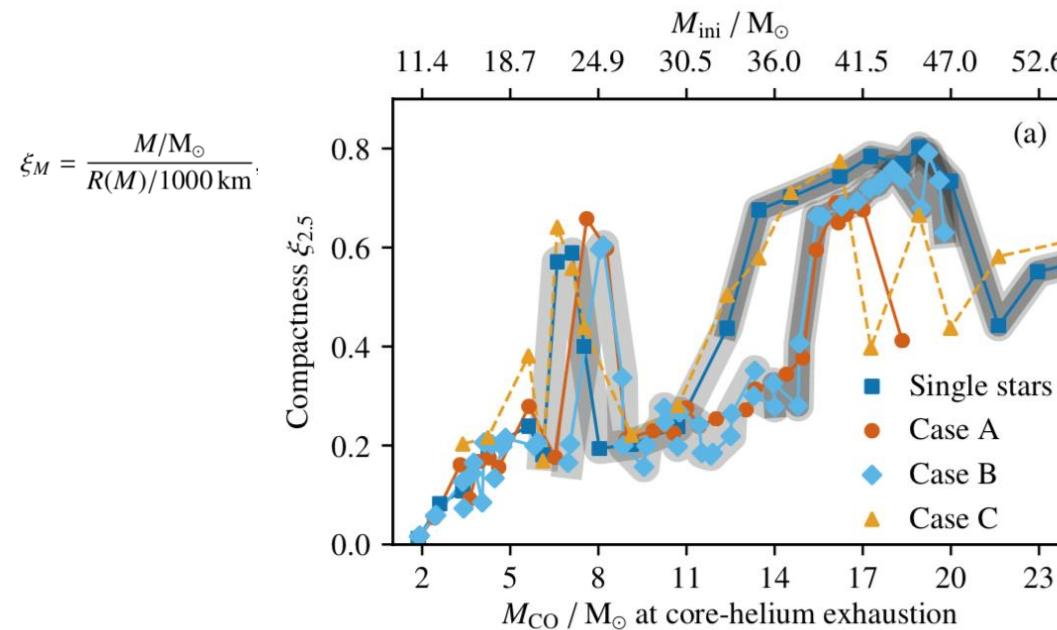
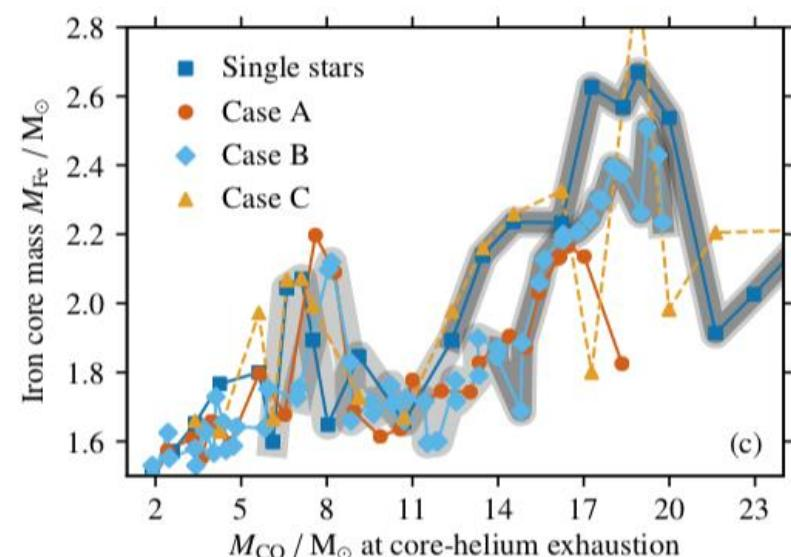
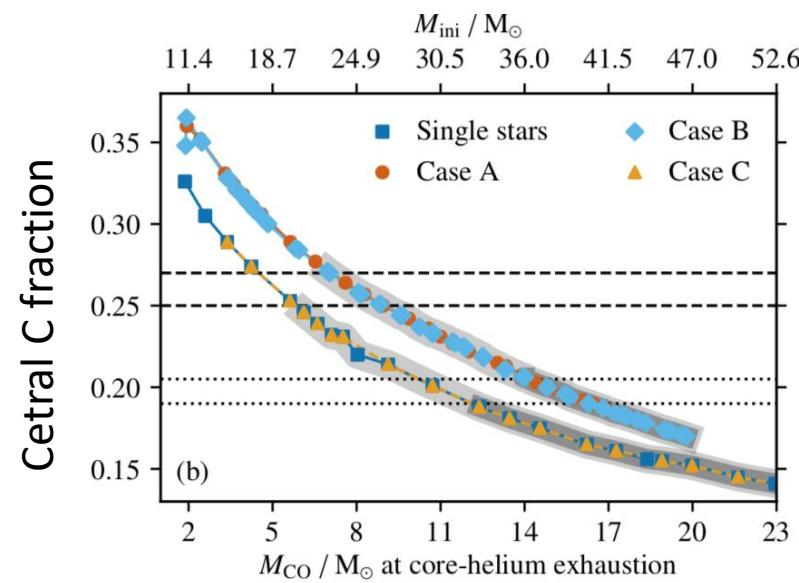
Binary evolution-- account for the majority of star mysteries, and produce important objects

Han+, 2020, RAA, 20, 161

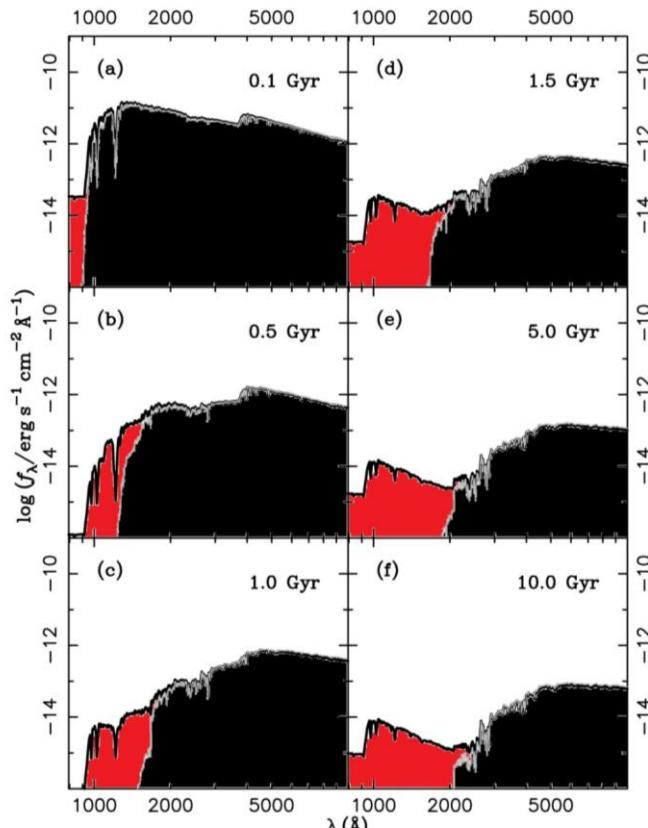


Impact on pre-supernova structure and compact object mass

Schneider+, 2021, A&A, 645, A5

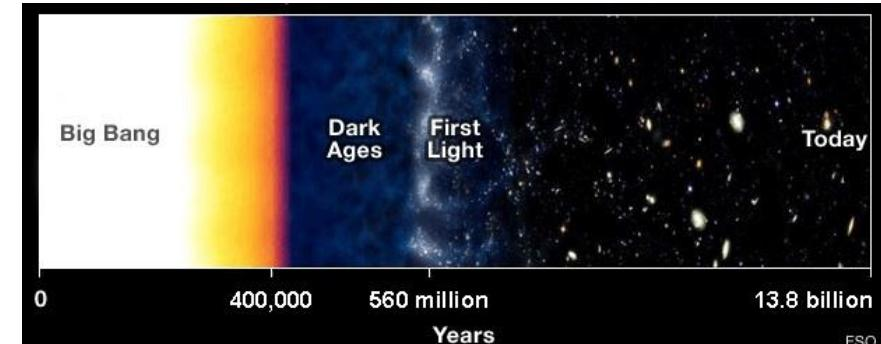


UV radiation of early type galaxies, cosmic reionization

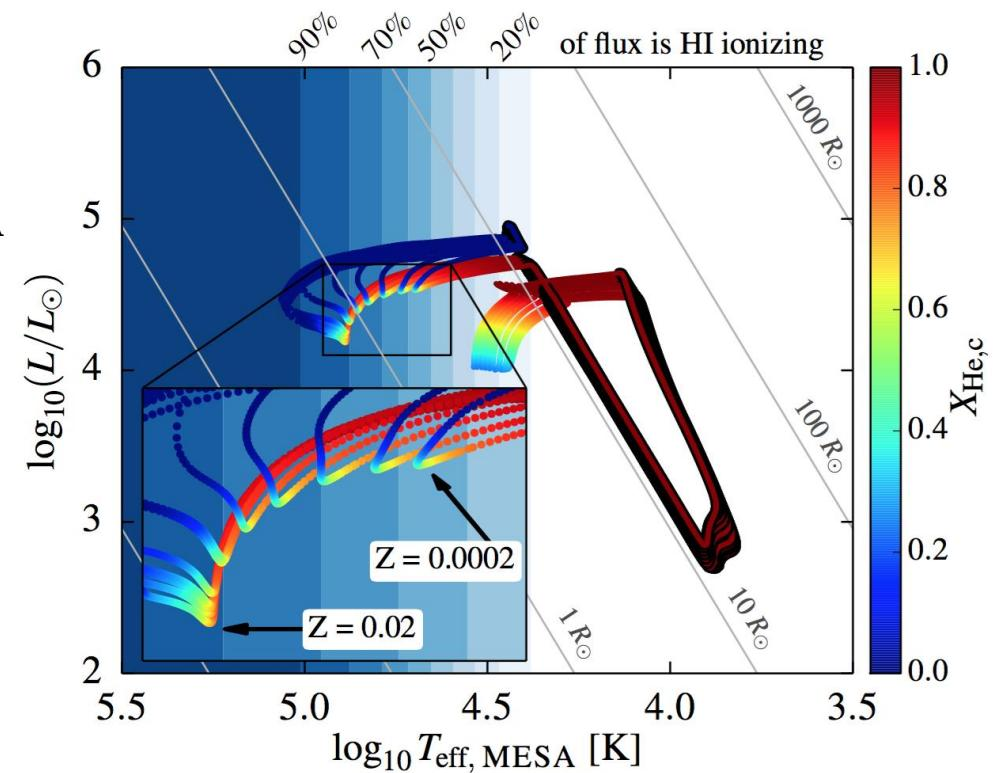


Han+, 2007, MNRAS

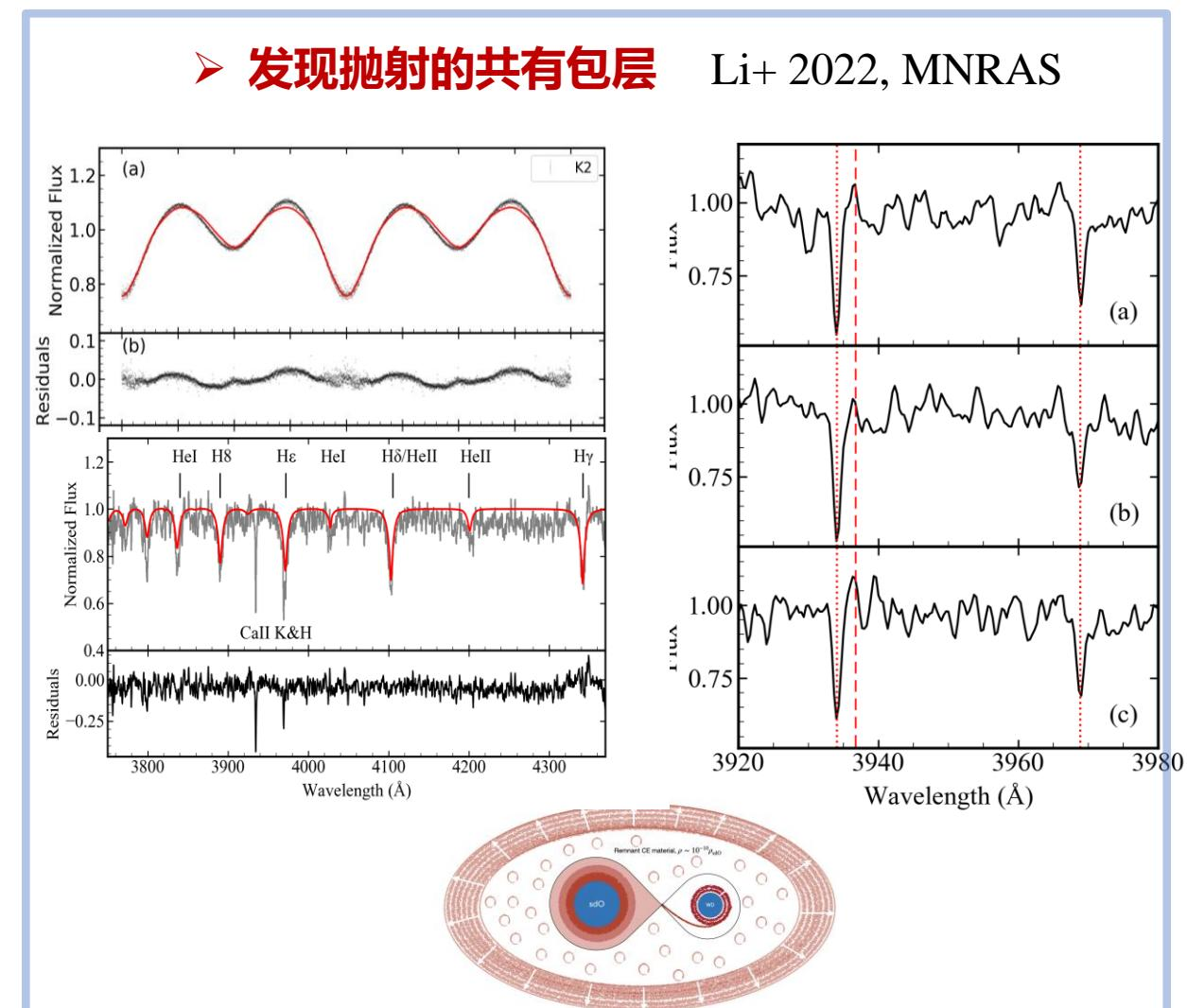
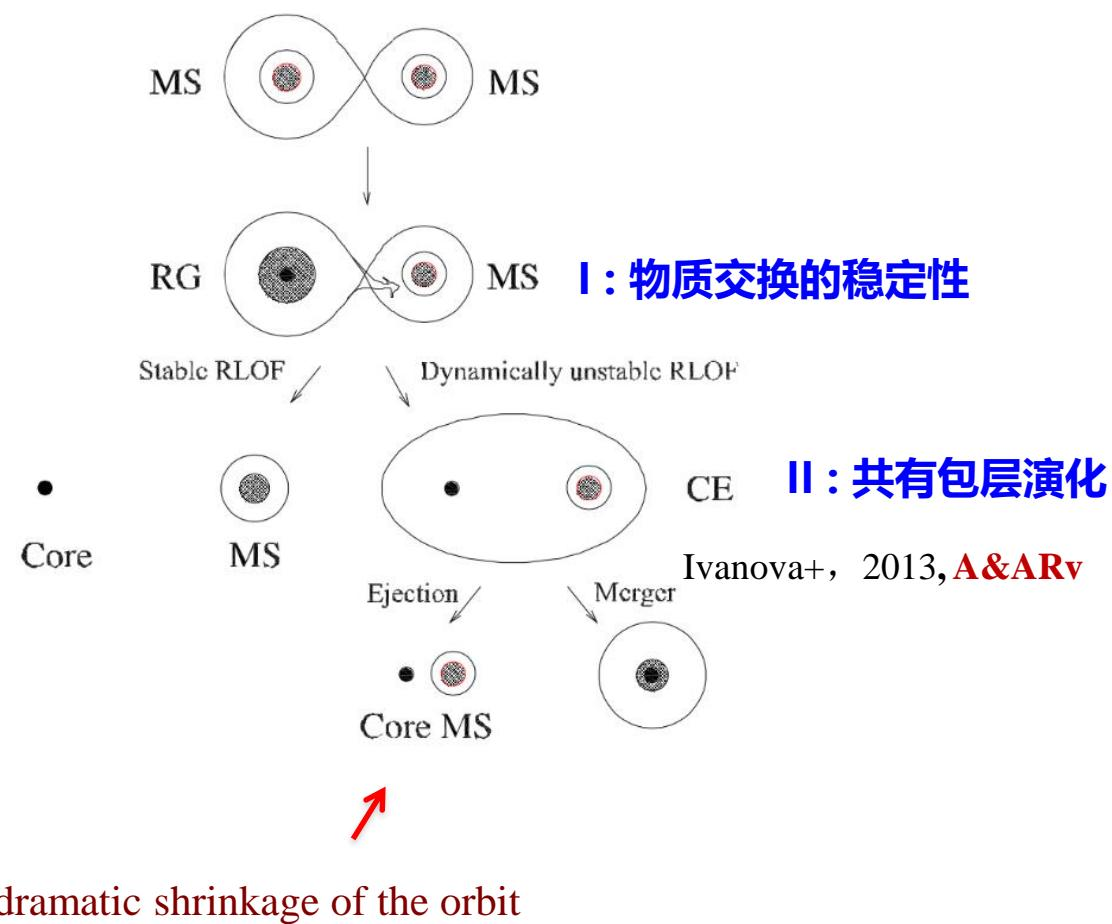
$$\begin{aligned}
 \eta &= \frac{f_{\text{strip}}}{f_{\text{WR, } 60 M_{\odot}}} \times \frac{Q_{0, \text{strip}}}{Q_{0, \text{WR}}} \times \frac{\Delta t_{\text{strip}}}{\Delta t_{\text{WR}}} \times \left(\frac{M_{\text{strip, init}}}{M_{\text{WR, init}}} \right)^{-2.35} \\
 &= \frac{0.33}{1.0} \times \frac{1.19 \times 10^{48} \text{ s}^{-1}}{2.8 \times 10^{49} \text{ s}^{-1}} \times \frac{1.2 \text{ Myr}}{0.4 \text{ Myr}} \times \left(\frac{12 M_{\odot}}{60 M_{\odot}} \right)^{-2.35} \approx 1.8
 \end{aligned}$$



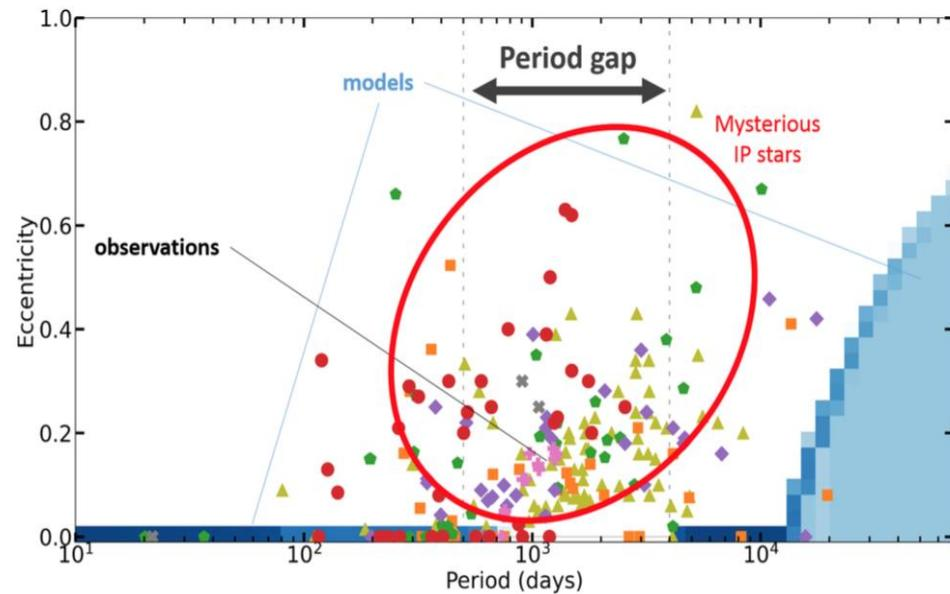
Gotberg+, 2017, A&A



Key uncertainties in modeling binary evolution

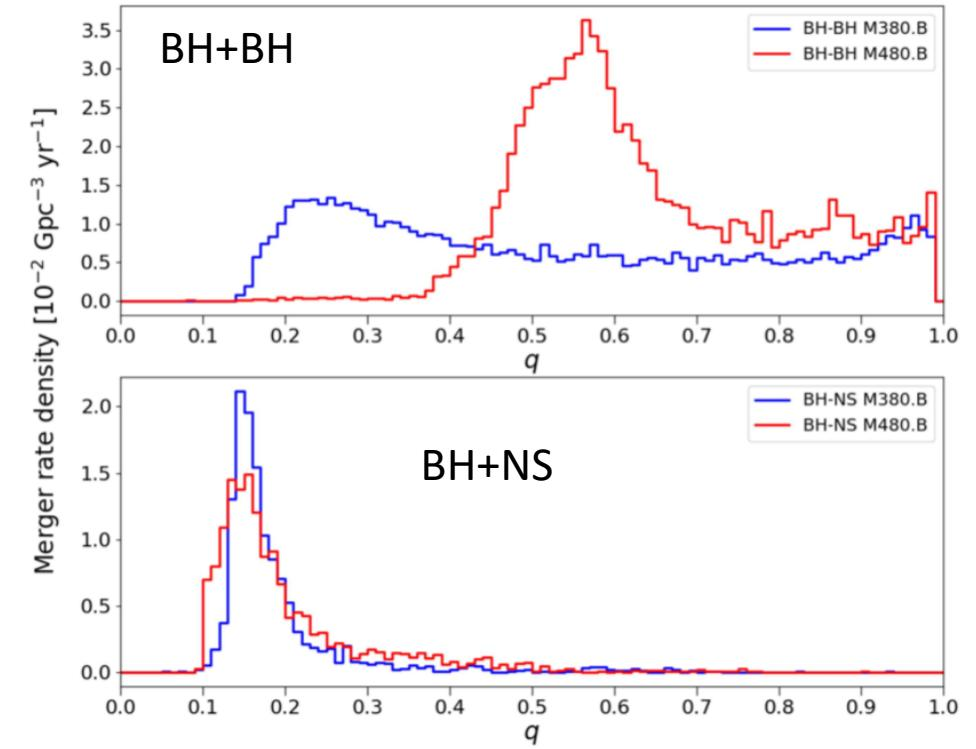


✧ discrepancy between theory and observations



✧ cannot predict observations accurately

Olejak, Belczynski, Ivanova, 2021, A&A, 651, A100



Red: Revised Criterion (Pavlovskii+, 2017)

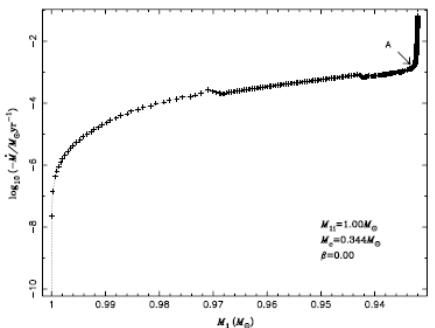
Blue: StarTrack standard

Belczynski et al., 2002, ApJ, 572, 407

物质交换的稳定性

寻找物质转移速率急剧上升点出现时的物理参数

Chen & Han, MNRAS, 2008



修改方程组，使其可以描述更短时标上恒星的变化

Ge+ 2010-2022系列论文

$$\frac{d \ln P}{dm} = -\frac{Gm}{4\pi r^4 P}, \quad \text{流体静力学平衡}$$

$$\frac{dr^2}{dm} = \frac{1}{2\pi r\rho}, \quad \text{质量分布}$$

$$\frac{d \ln T}{dm} = \frac{d \ln P}{dm} \nabla \quad \text{能量传递}$$

$$\frac{dL}{dm} = \epsilon - \epsilon_\nu - C_p T \left(\frac{d \ln T}{dt} - \nabla_a \frac{d \ln P}{dt} \right) \quad \text{能量守恒}$$

恒星结构的基本方程组

$$\frac{d \ln P}{dm} = -\frac{Gm}{4\pi r^4 P},$$

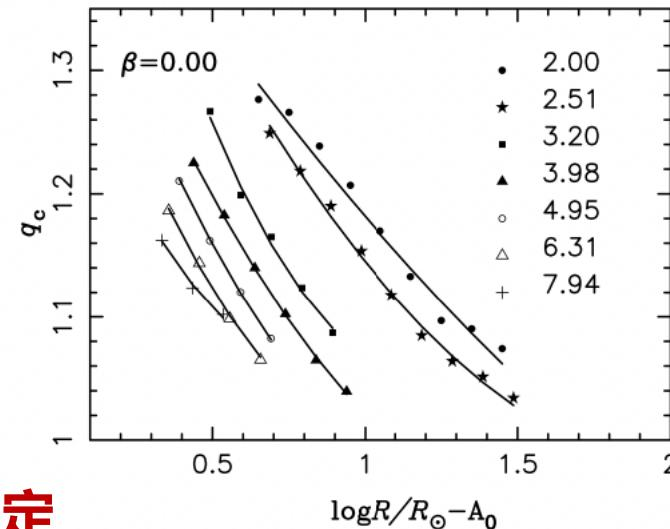
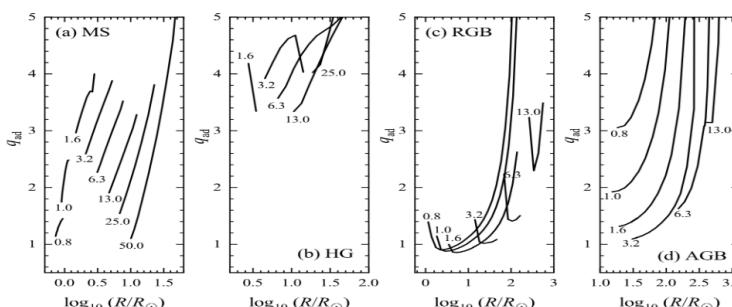
$$\frac{dr^2}{dm} = \frac{1}{2\pi r\rho}, \quad \text{绝热}$$

$$s' \equiv ds/dt = s(m) - s_0(m) = 0,$$

$$X' \equiv dX/dt = X(m) - X_0(m) = 0.$$

绝热物质损失模型

Han+, 2021, RAA



双星物质交换更容易稳定

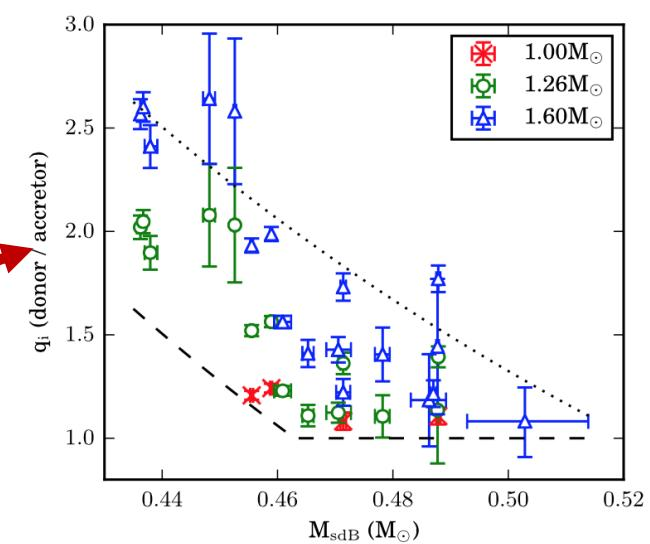
特别地，红巨星支和渐进巨星支恒星：

以往 $q_c = M_1/M_2 < 1$ 全部不稳定

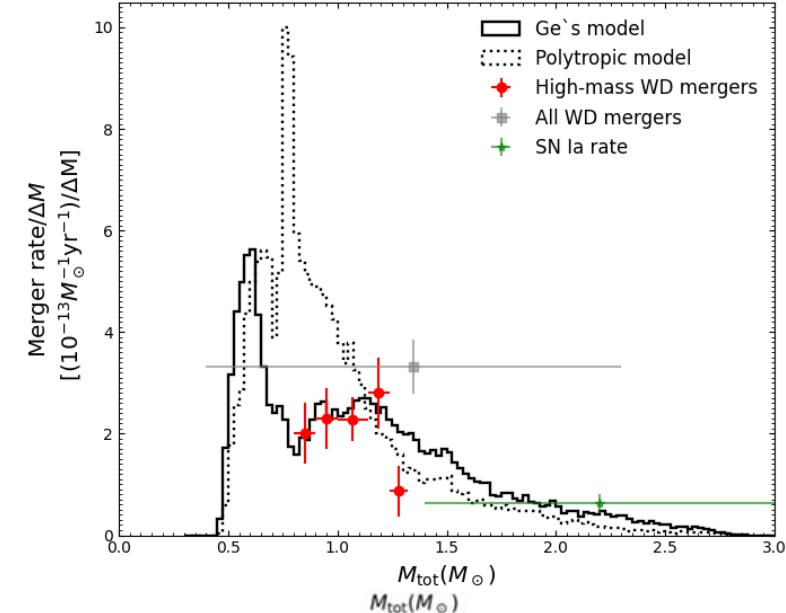
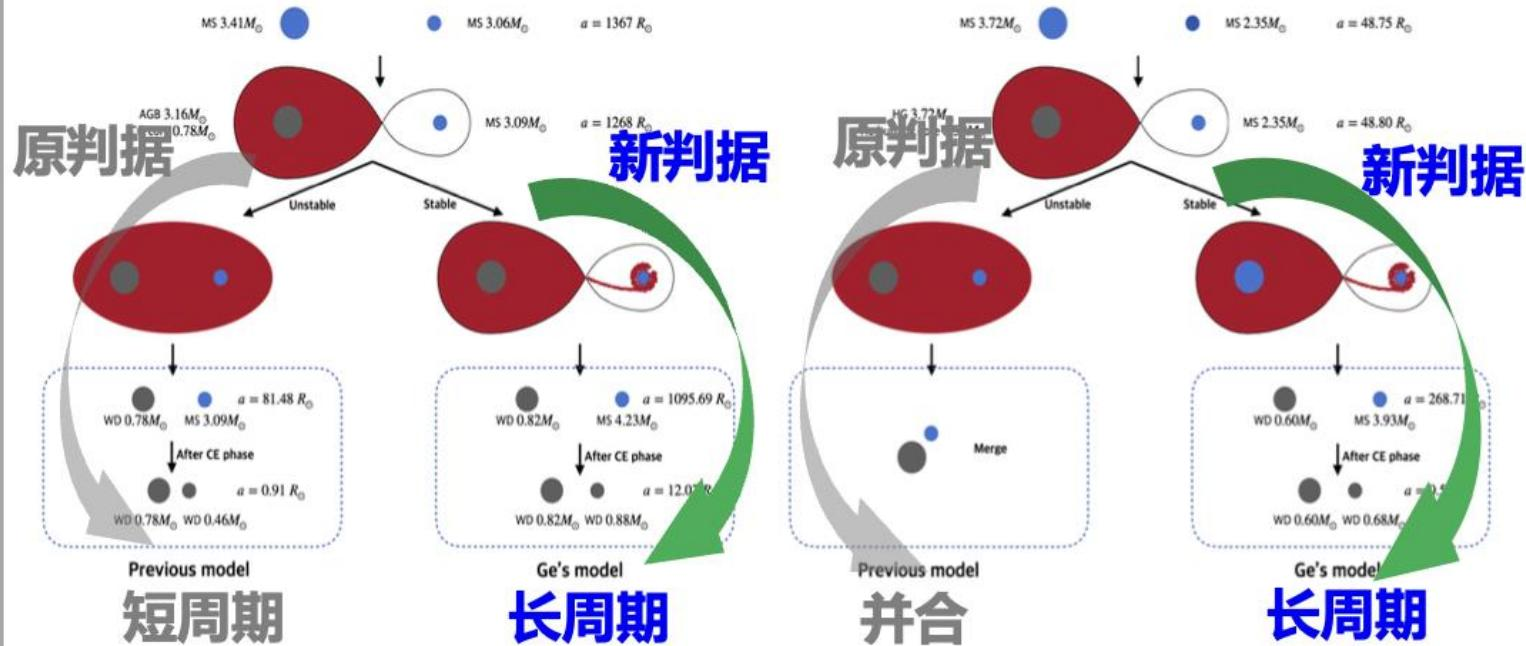
现在 $q_c = M_1/M_2 \sim 1 - 5$ 部分稳定，部分不稳定

观测限制

Vos+2019, MNRAS

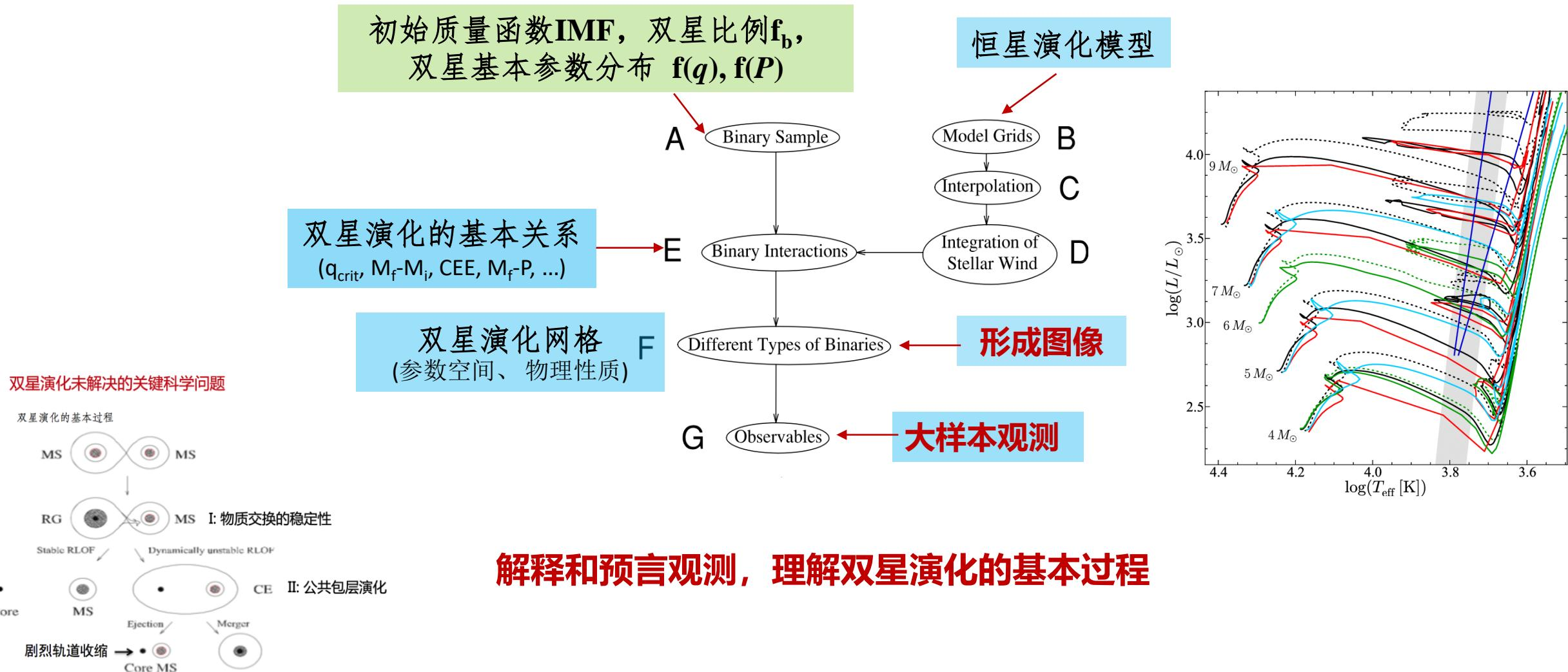


双白矮星的形成通道发生显著改变



双星星族合成

– 大数据时代研究特殊恒星形成的主要方法



双星比例和双星族的统计性质

- **双星比例和金属丰度的关系**

anti-correlation (Raghavan+ 2010, Moe+ 2019) or

positive correlation (Moe+ 2013) ?

- **质量比分布**

low- q weighted (Duquennoy+ 1991)

flat (Raghavan+ 2010)

double peaks (Glodberg+ 2013)

power-law (Duchene+ 2013)

- **周期分布**

dependant on stellar mass ? (Moe+ 2017)

- 不同环境双星族的统计性质：为双星星族合成提供基本输入
- 双星演化形成的关键天体：研究双星演化基本过程

重复观测

课题的研究内容和目标

- 根据CSST的性能指标，对CSST在双星科学重要问题上的潜力进行预研究；
- 发展一系列基于CSST多色测光和无缝光谱数据识别各类双星的算法和恒星或双星参数测量算法。

课题下设五个子课题：

- **双星统计研究** (子课题负责人：韩占文 云台)

对太阳邻域、星团和近邻星系中的双星比例、基本参数分布进行预研究，评估CSST在此研究方面的能力。

- **光谱双星** (子课题负责人：陈雪飞 云台)

研究光谱双星的质量比、光谱双星在不同环境下的参数分布。

- **双星演化形成的特殊天体** (子课题负责人：吕国梁 新疆大学)

大质量双星、蓝离散星、蓝水平分支星/热亚矮星、后AGB双星、主序-白矮双星、激变变星、共生星、行星状星云中心双星、非相互作用黑洞/中子星双星

- **(吸积) 白矮星及相关天体** (子课题负责人：陈海亮 云台)

- **超高速星** (子课题负责人：李荫碧 国台)

研究进展

I、通过CSST多色测光识别主序星双星



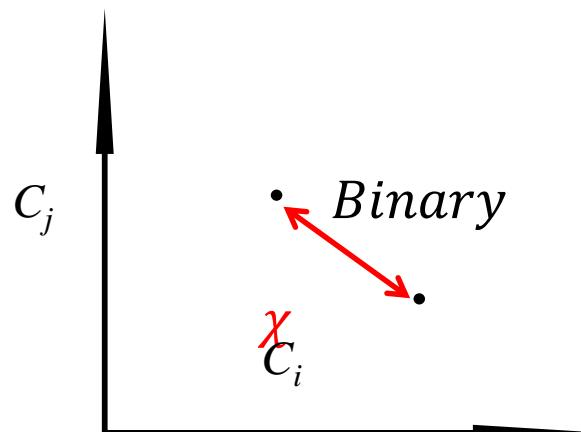
Single Star -- M_1
 $q = \frac{M_2}{M_1} = (0,1]$ $\Delta \log M_1 = 0.1$
-- M_2

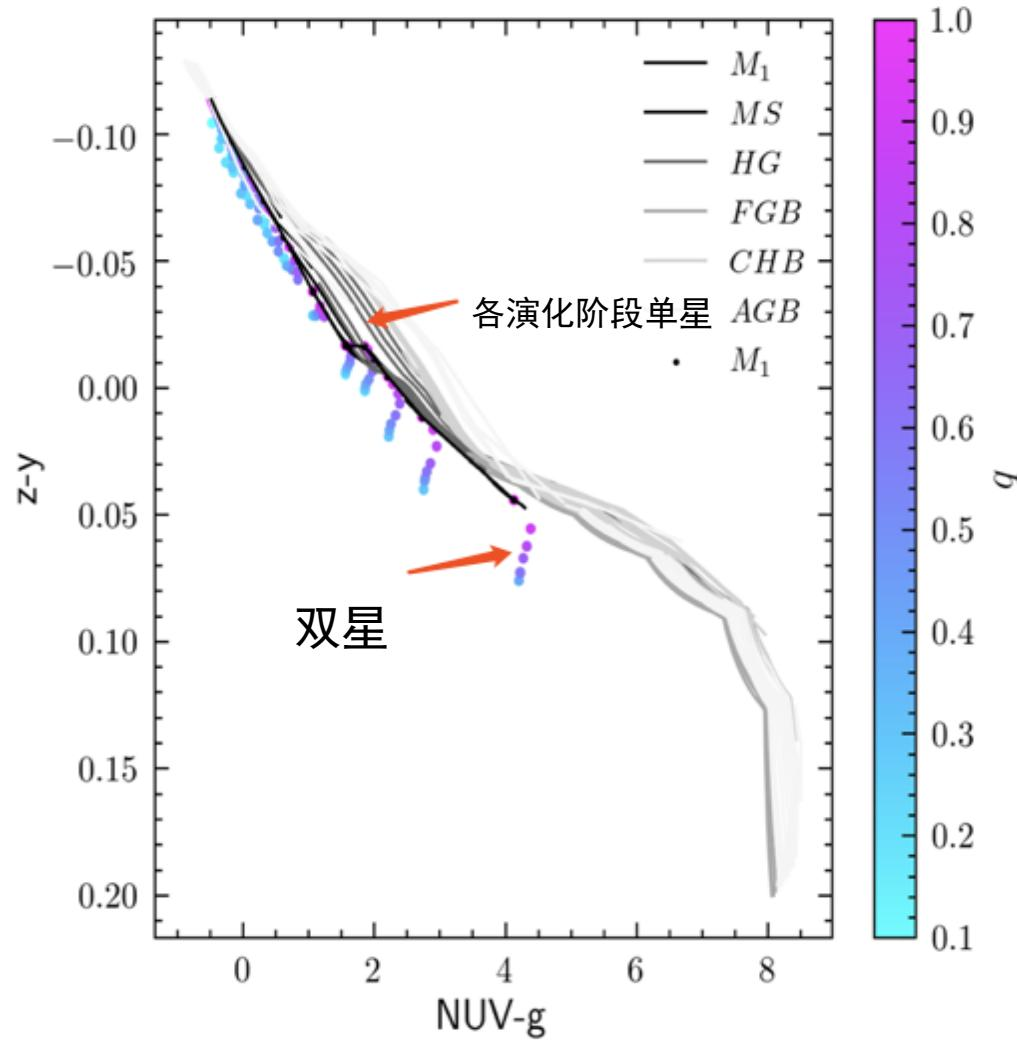
-- Binary star

$$C_i = mag_{band1} - mag_{band2}$$
$$C_j = mag_{band3} - mag_{band4}$$

$$\Delta C_i = C_{i_{single}} - C_{i_{binary}}$$
$$\Delta C_j = C_{j_{single}} - C_{j_{binary}}$$

$$\chi^2 = \Delta C_i^2 + \Delta C_j^2$$

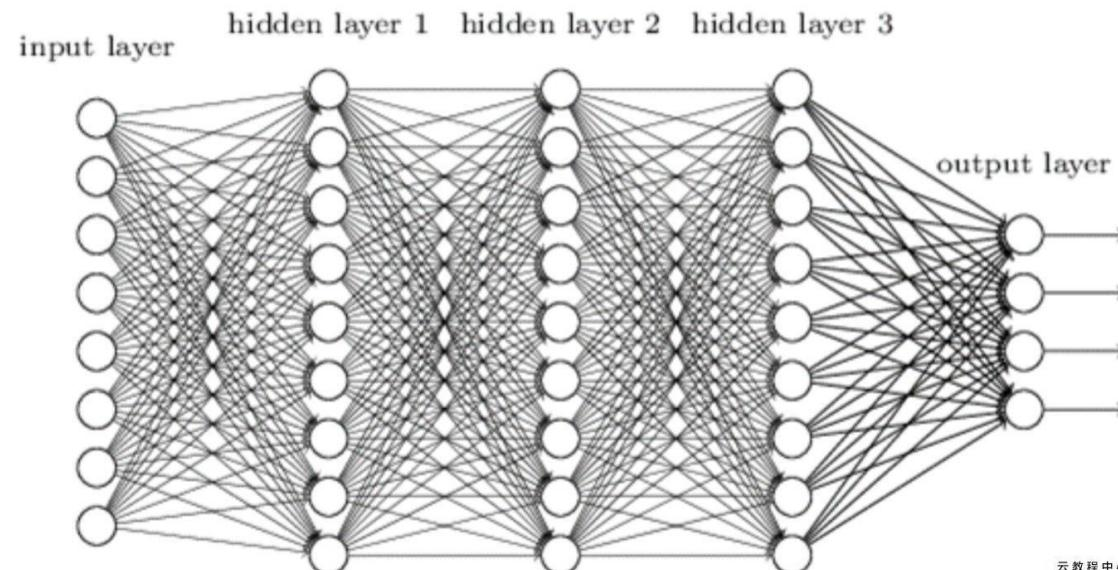
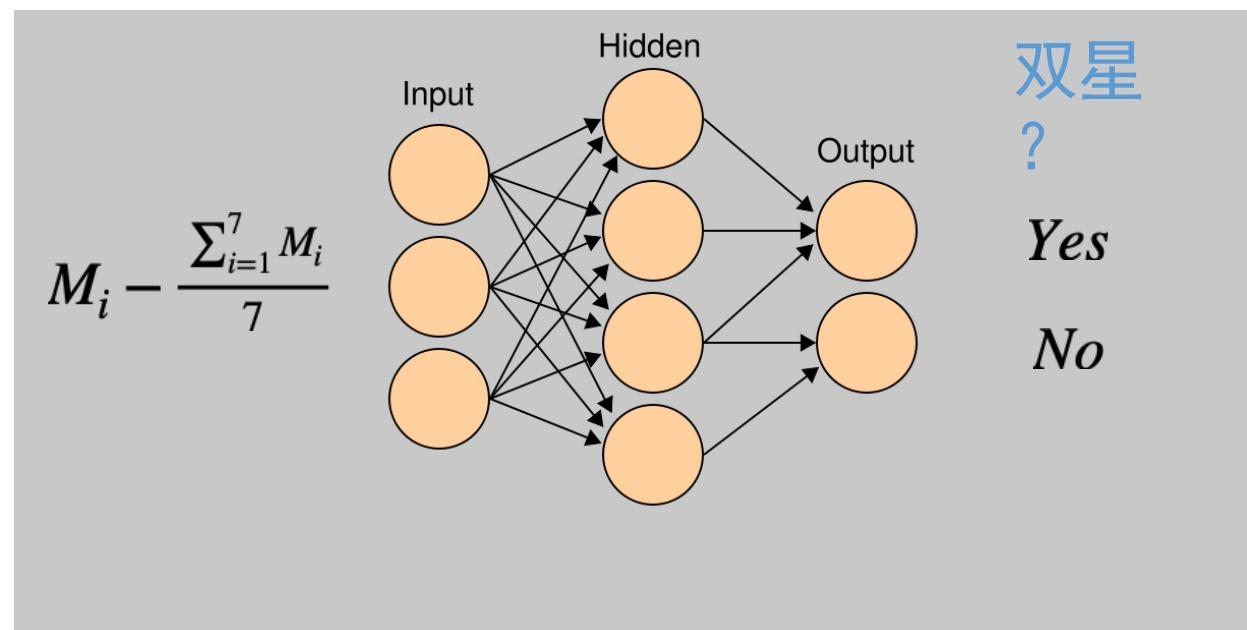




共11组颜色比较容易将
小质量双星和单星分开。

NUV-u	z-y	u-g	z-y
NUV-g	z-y	u-r	z-y
NUV-r	z-y	u-i	z-y
NUV-i	z-y	u-z	z-y
NUV-z	z-y	u-y	z-y
NUV-y	z-y		

	binary	M1	M2
NUV			
u			
g			
r			
i			
z			
y			



双星

?

Yes

No

Prediction Outcome

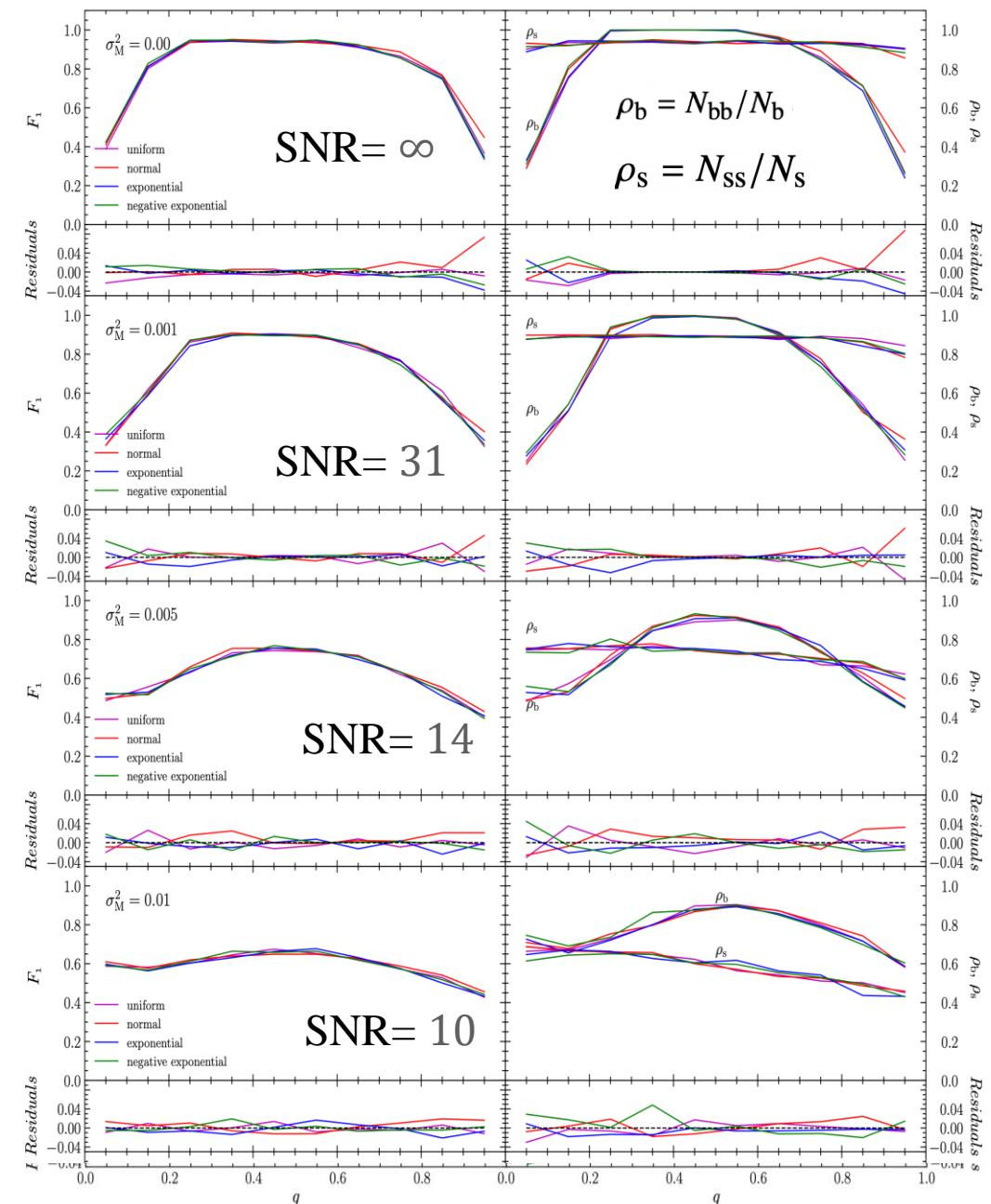
		Prediction Outcome	
		BB N_{bb}	BS N_{bs}
Actual Value	BB N_{bb}		
	SB N_{sb}	SS N_{ss}	
B		S	

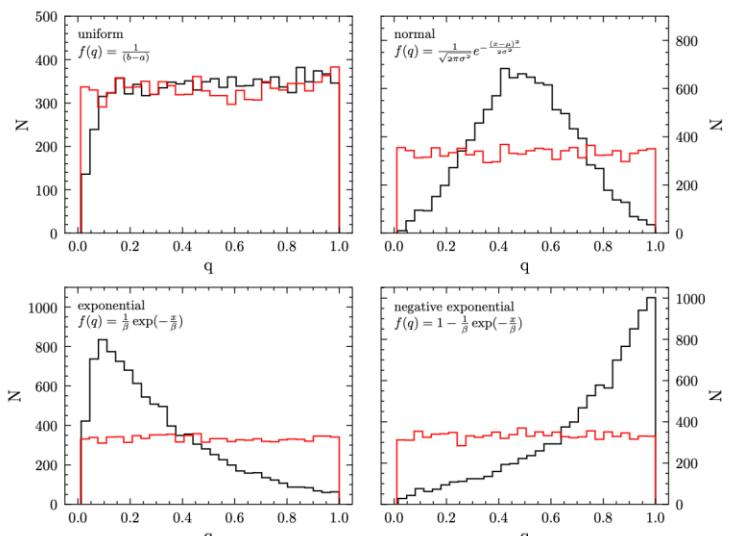
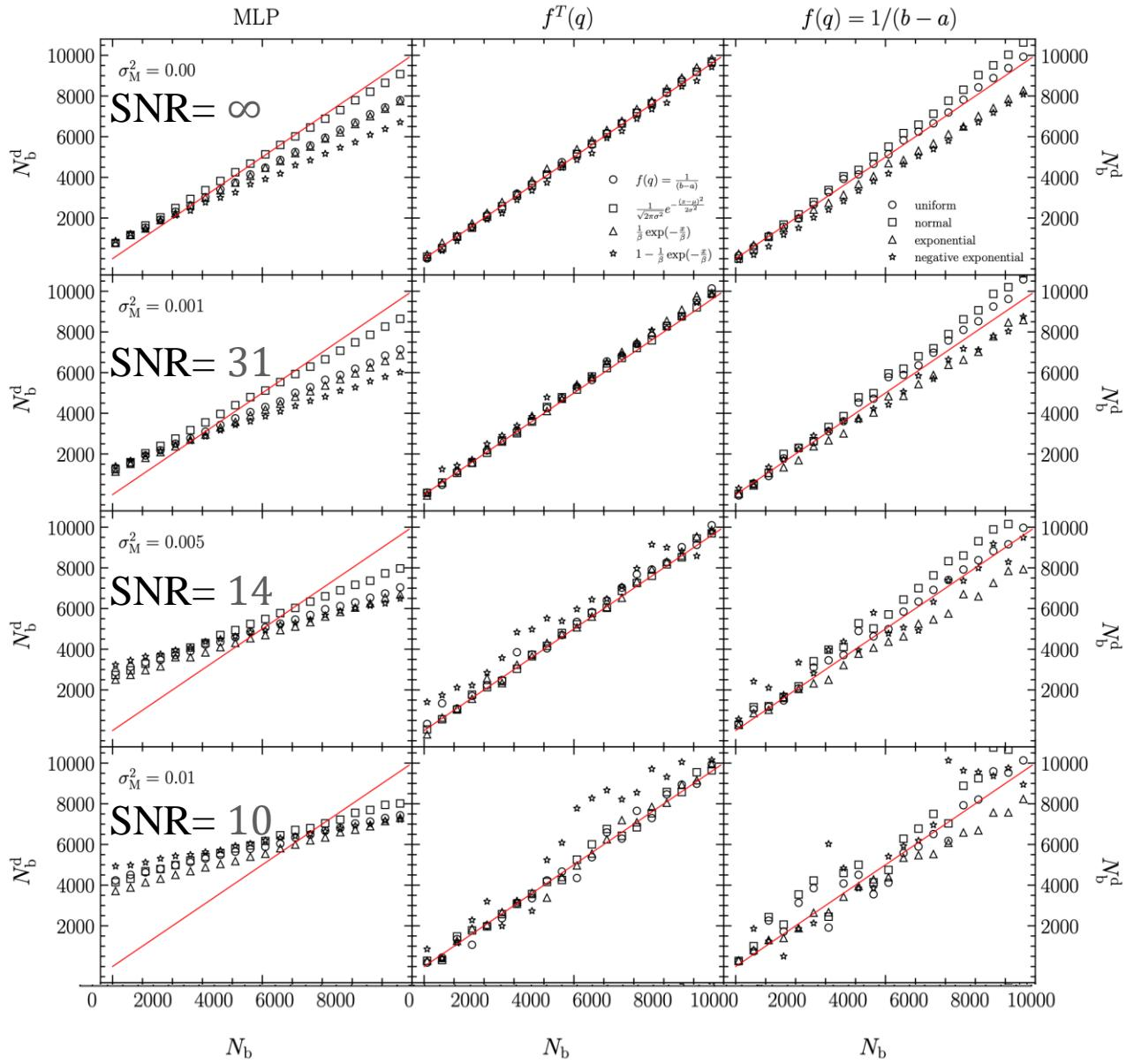
$$B' \\ N_b = N_{bb} + N_{bs} \\ N' \\ N_s = N_{sb} + N_{ss}$$

$$F_1 = \frac{2 \times P \times R}{P + R}$$

$$\text{精度 } P = N_{bb}/(N_{bb} + N_{sb})$$

$$\text{召回率 } R = N_{bb}/N_b$$

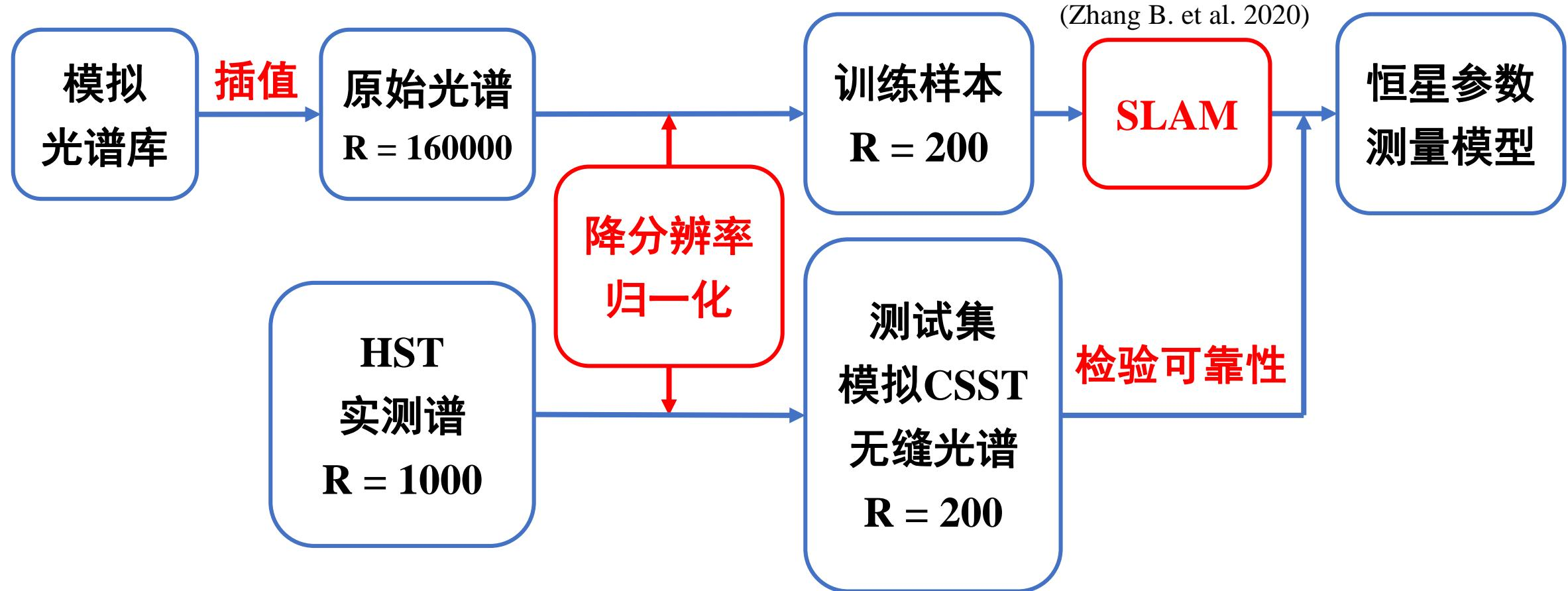




$$N_b = \frac{(1 - \rho_s)N - N_b^d}{1 - \rho_b - \rho_s},$$

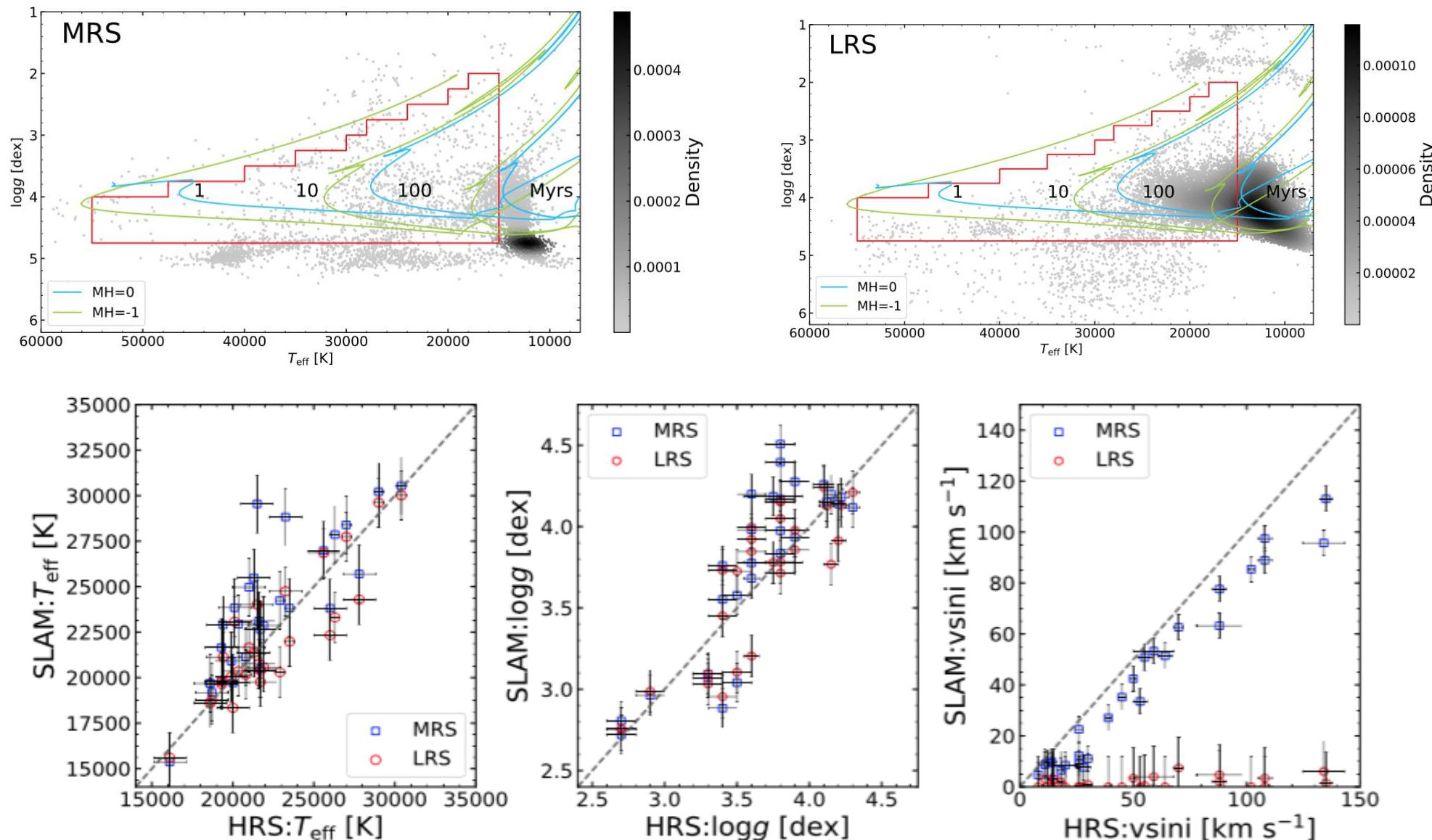
$$f_b = \frac{1 - \rho_s - f_b^d}{1 - \rho_b - \rho_s},$$

II、基于CSST无缝光谱估计恒星参数



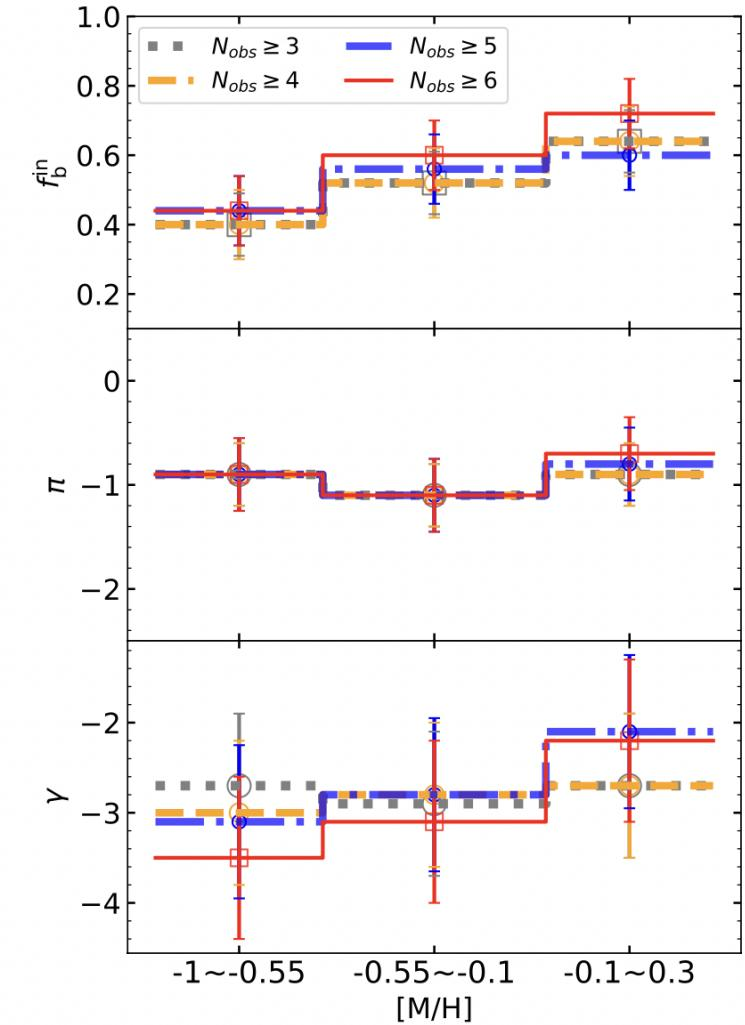
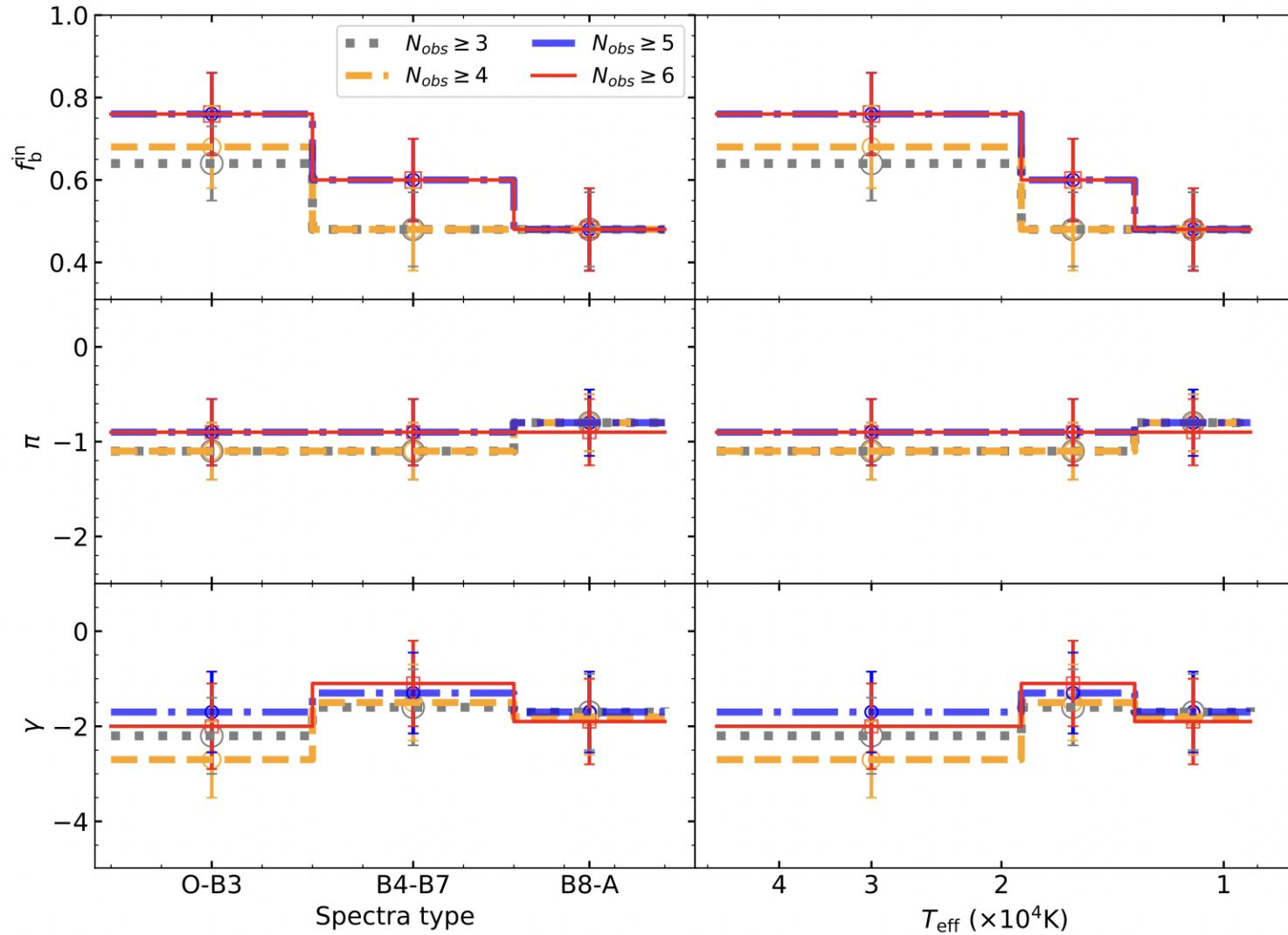
Stellar Labels of early-type stars from LAMOST MRS/LRS from machine learning (SLAM)

Guo et al. 2021, ApJS



The statistical properties of early-type stars from LAMOST DR8

Guo et al., 2022, A&A



POWR模拟光谱库 (The Potsdam Wolf-Rayet Models)

基于POWR恒星大气模型构建

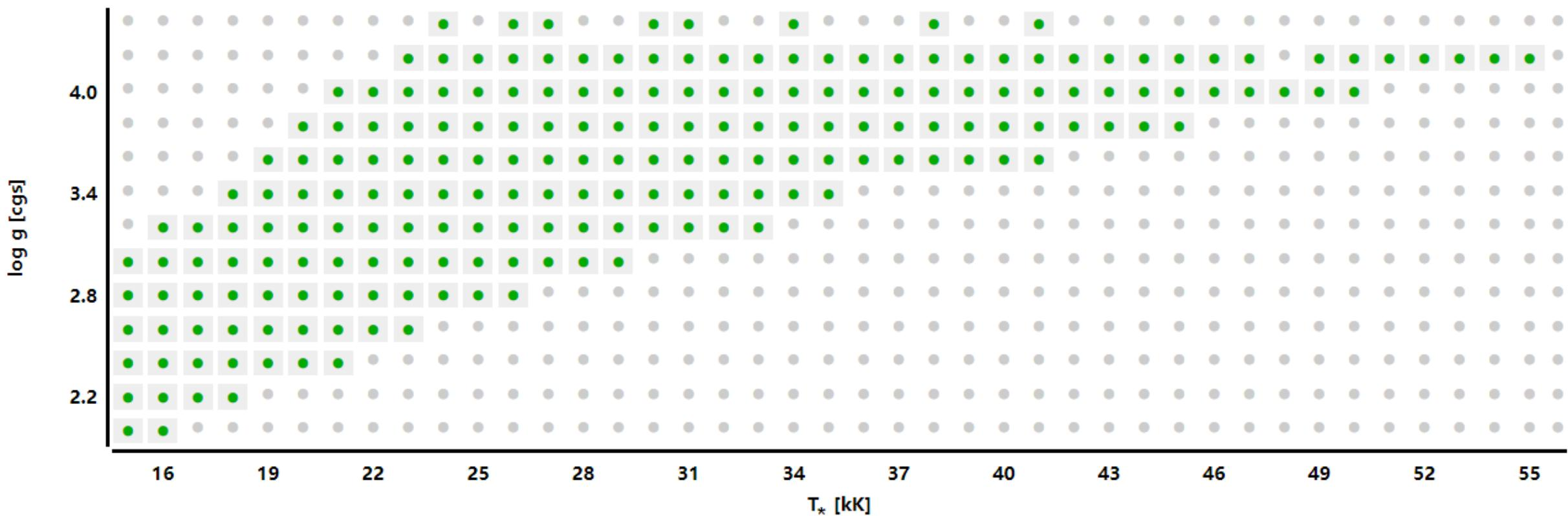
NLTE

球形扩散

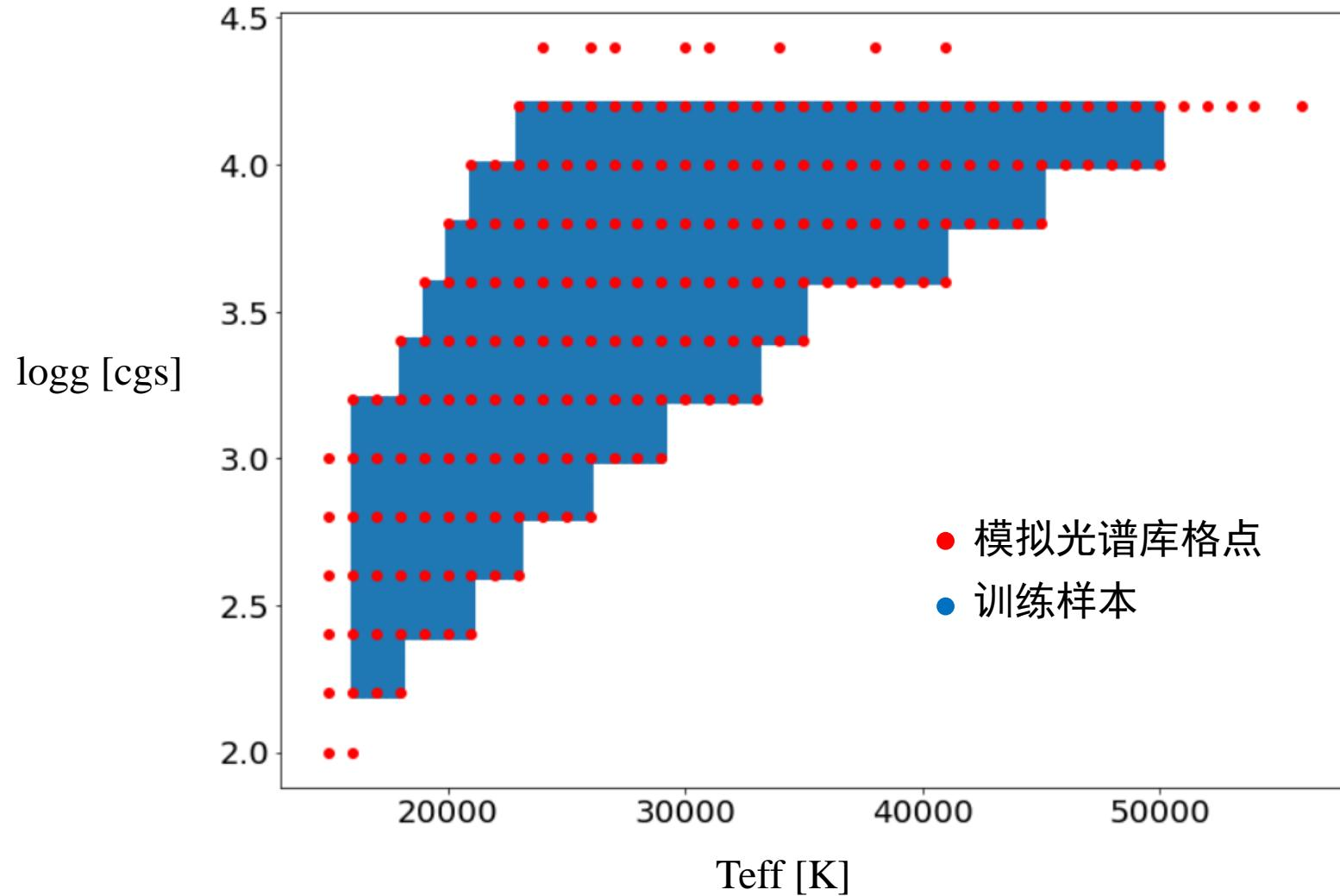
金属线覆盖

温度范围: 16000K – 55000K

波长范围: **覆盖了CSST (2550A – 10000A)**

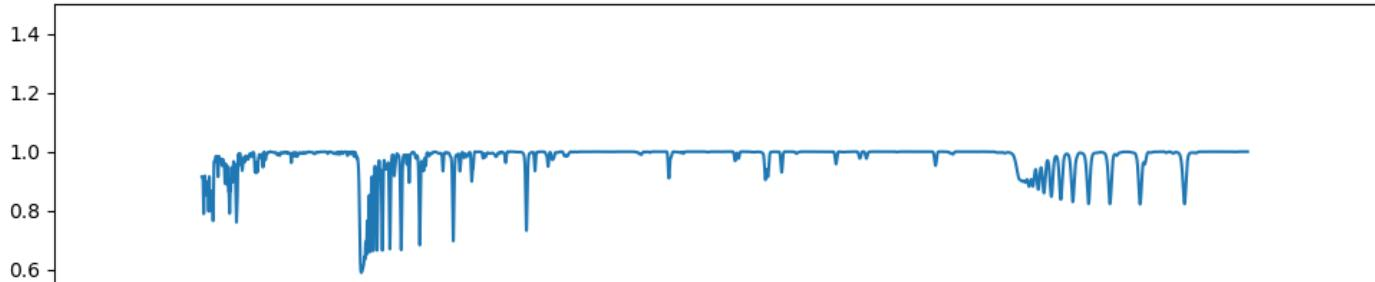


模拟光谱库格点分布及训练样本选取

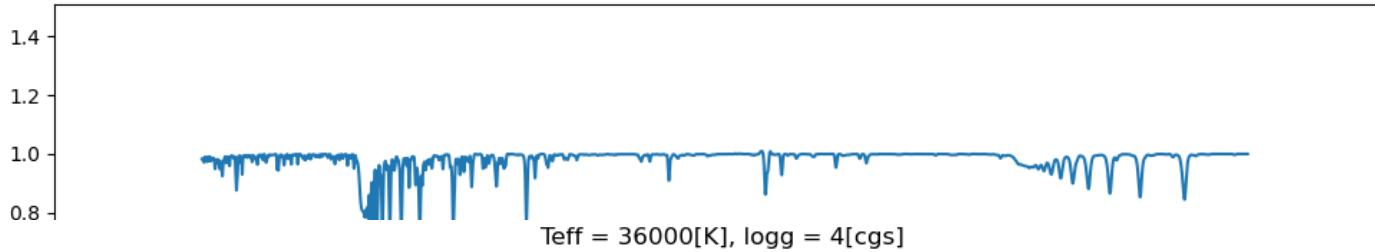


删除含有强发射线的光谱

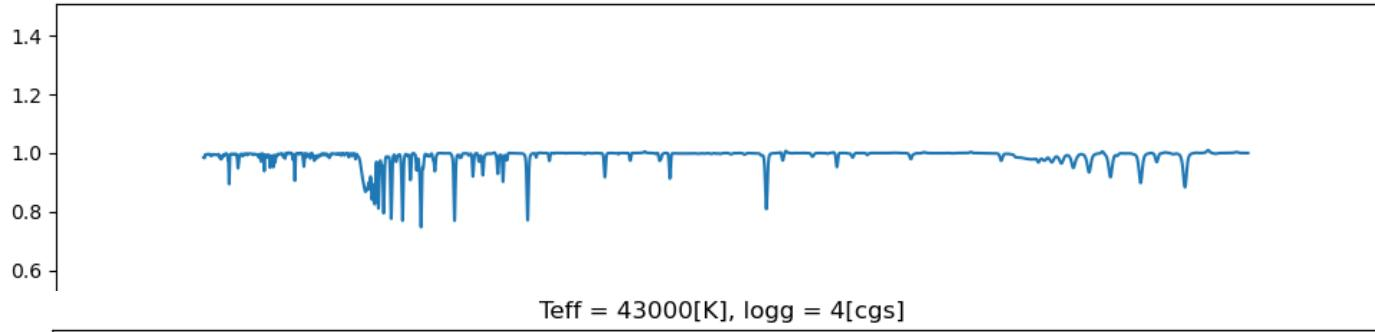
Teff = 15000[K], logg = 2[cgs]



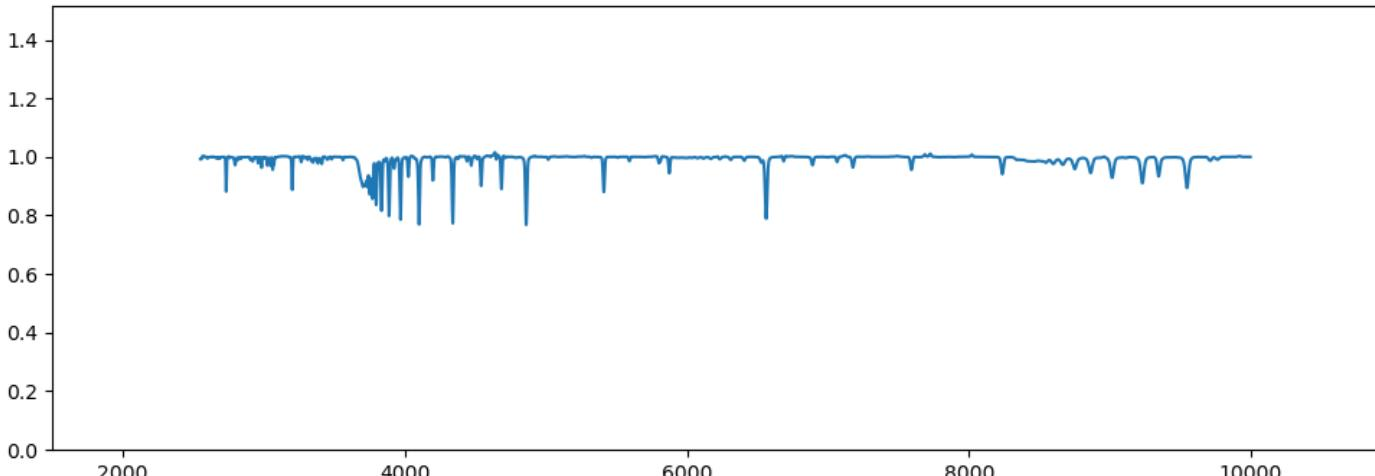
Teff = 25000[K], logg = 3[cgs]



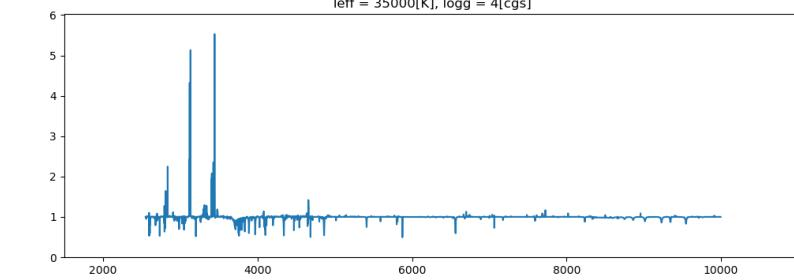
Teff = 36000[K], logg = 4[cgs]



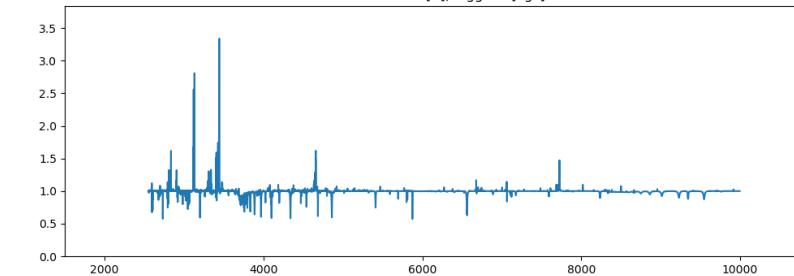
Teff = 43000[K], logg = 4[cgs]

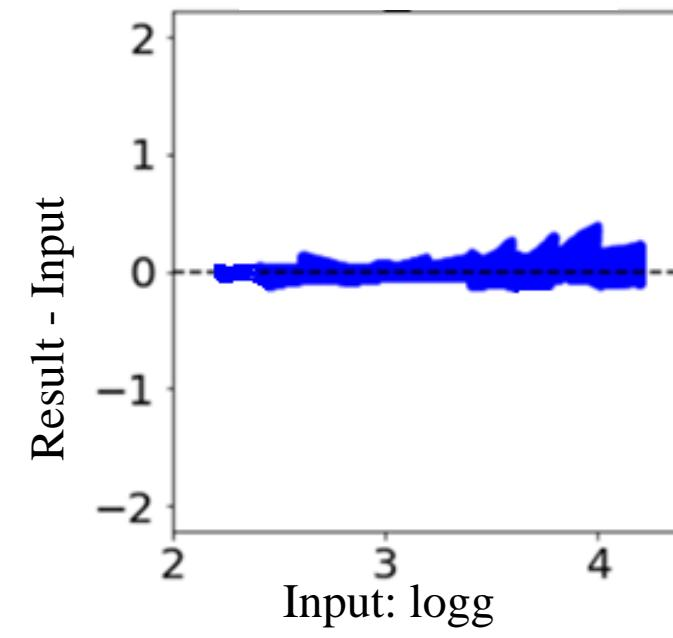
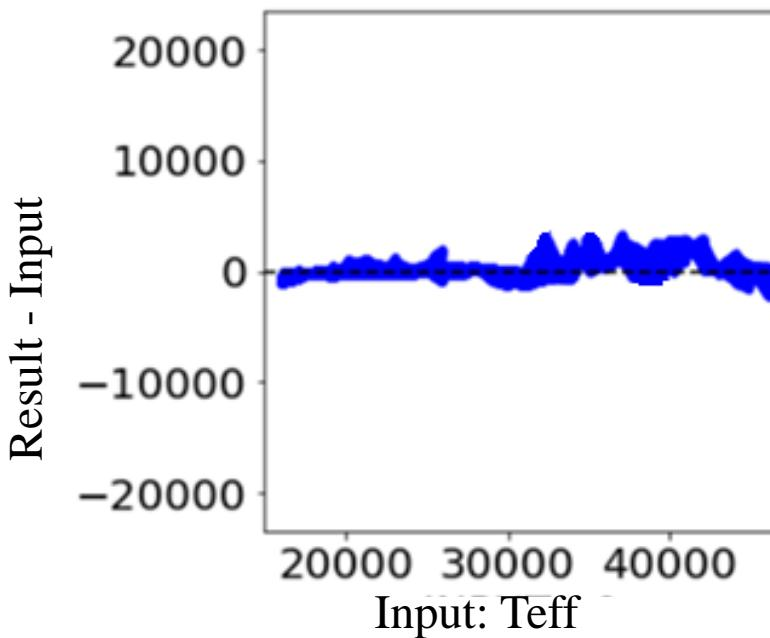
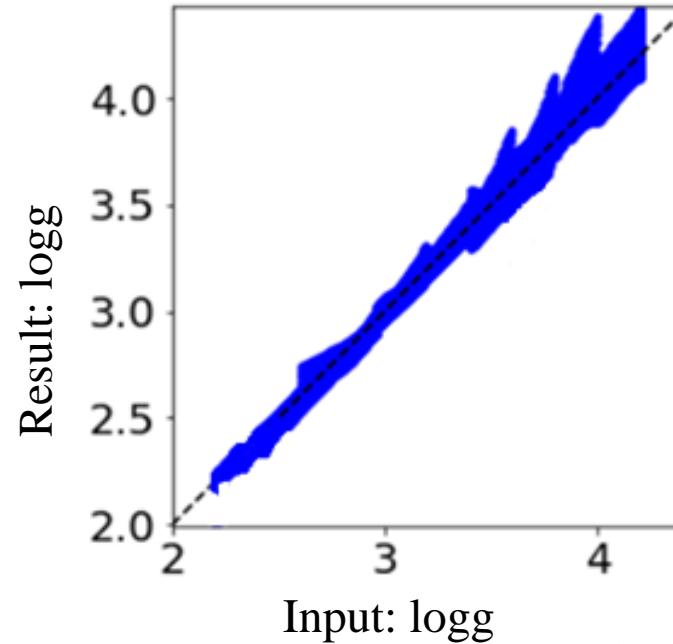
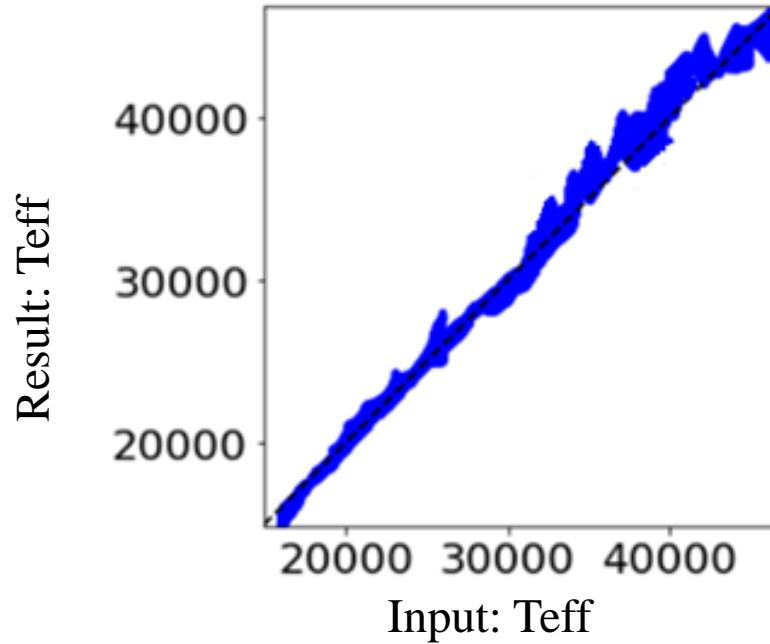


Teff = 35000[K], logg = 4[cgs]



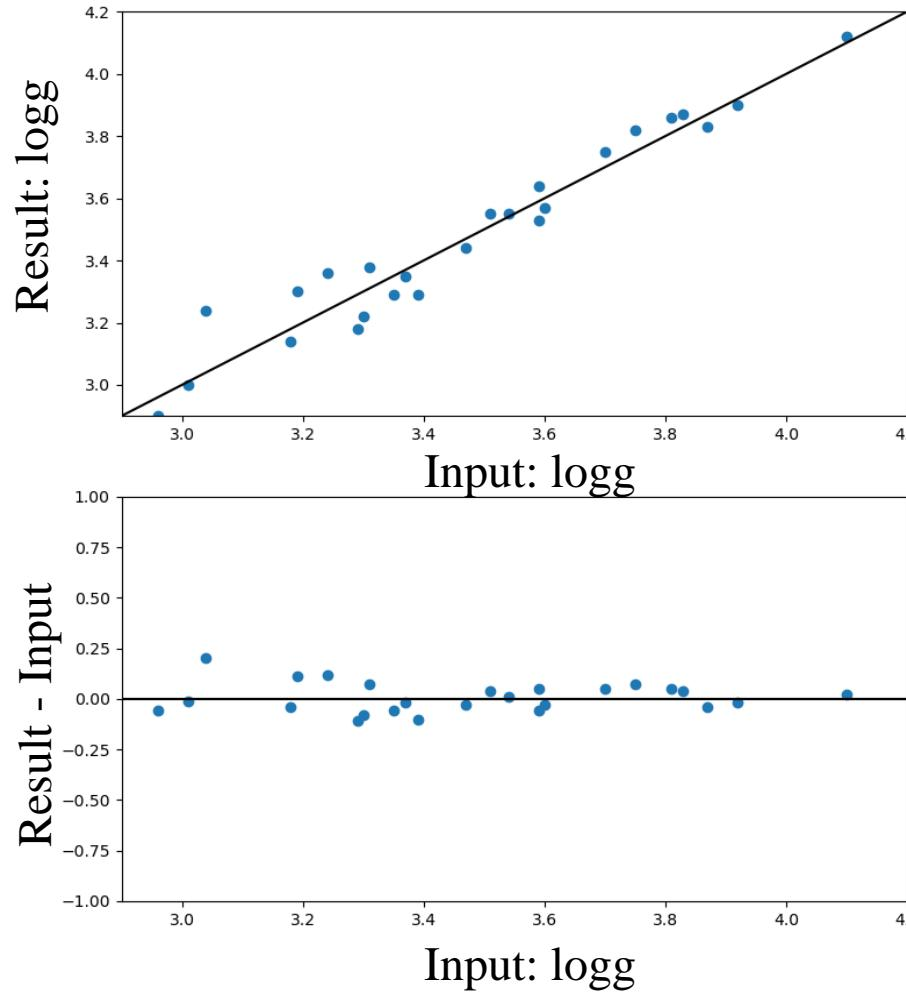
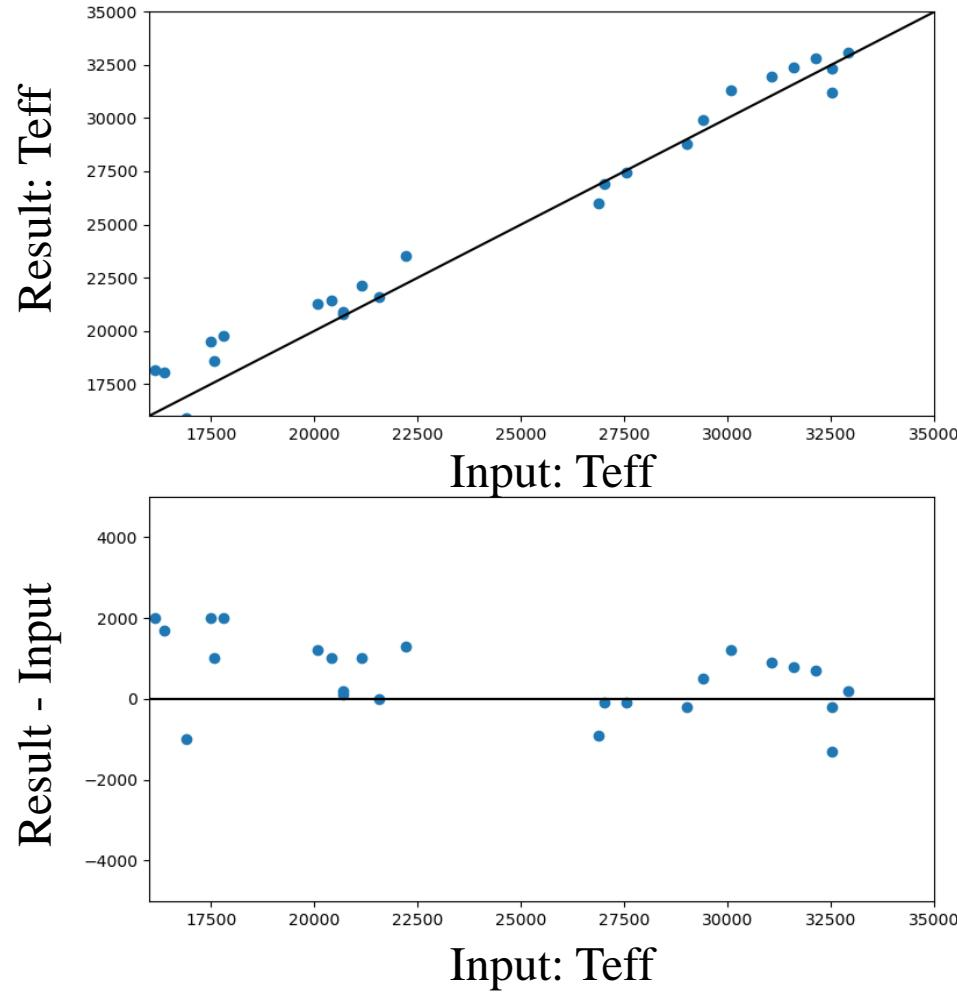
Teff = 41000[K], logg = 4[cgs]





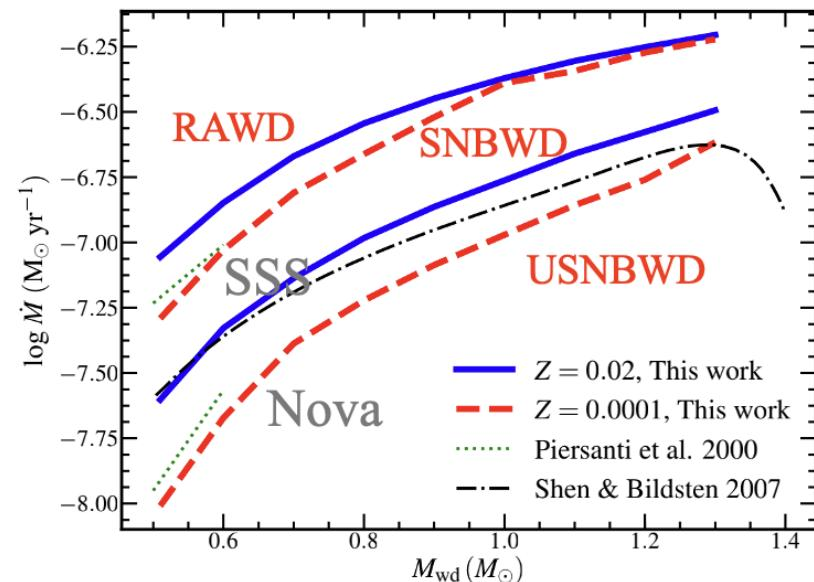
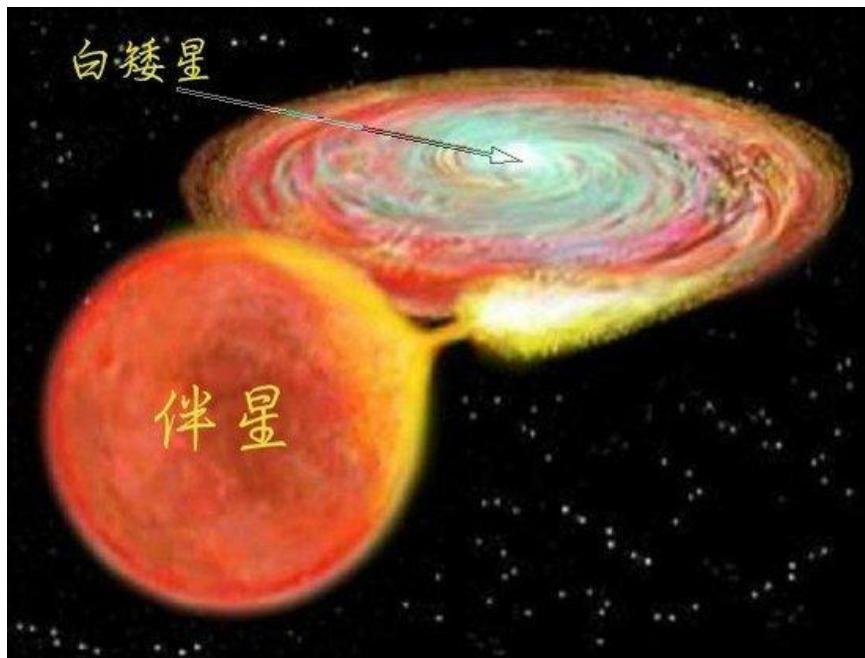
误差范围小于 9%

HST实测数据检验模型 (< 11%)



III、基于CSST测光系统寻找特殊双星

吸积白矮星



快速吸积白矮星(RAWD)
典型有效温度范围 $\sim 10^4 - 10^5$ K
紫外波段

稳定燃烧白矮星(SNBWD)
典型有效温度范围 $\sim 10^5 - 10^6$ K
极紫外波段

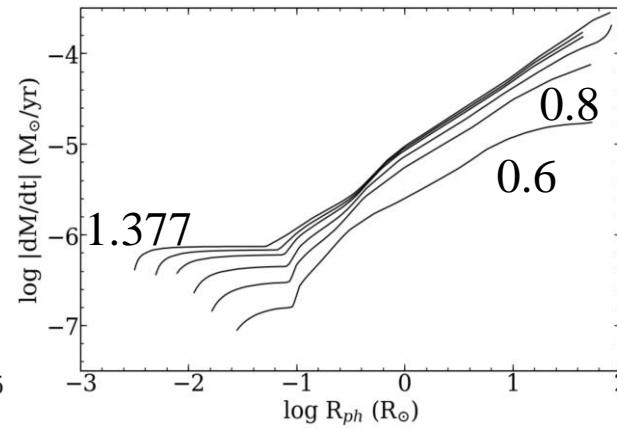
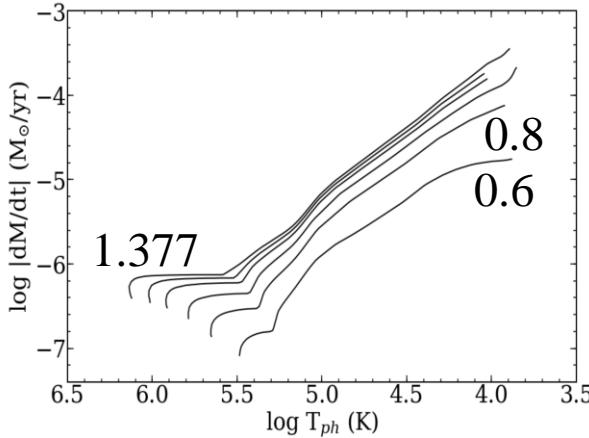
不稳定燃烧白矮星(USNBWD)

目前快速吸积白矮星尚未找到，观测稳定燃烧白矮星的数量也非常少。

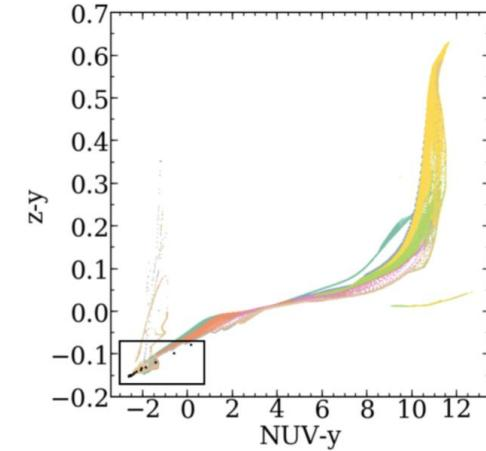
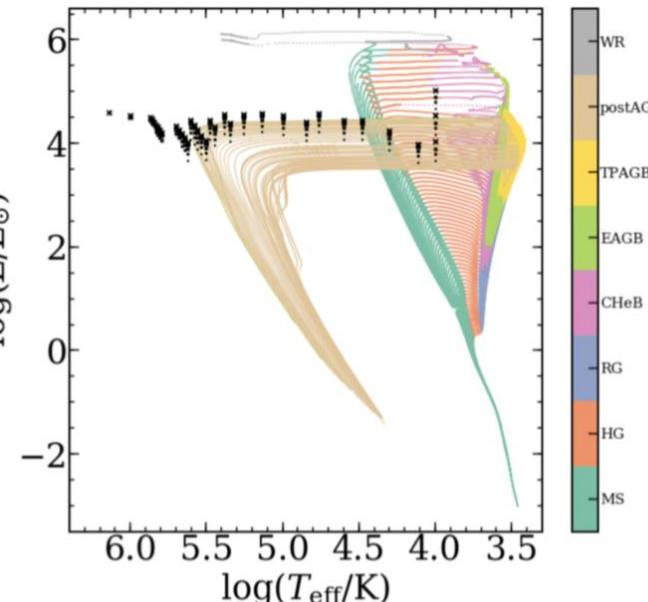
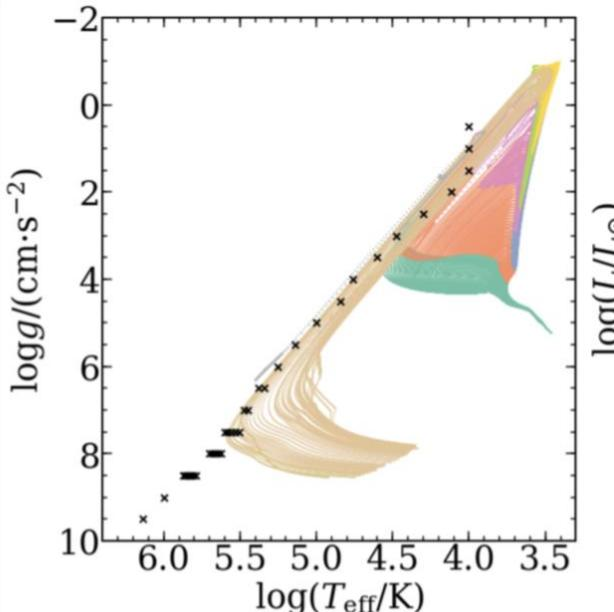
Ia型超新星、新星、激变变星

星系的化学演化、X-射线辐射、星系的电离源

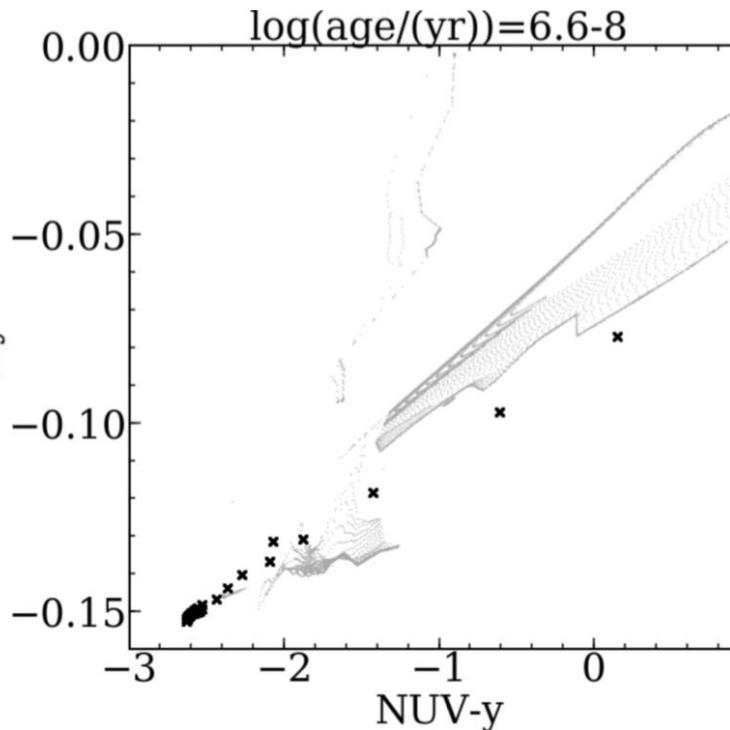
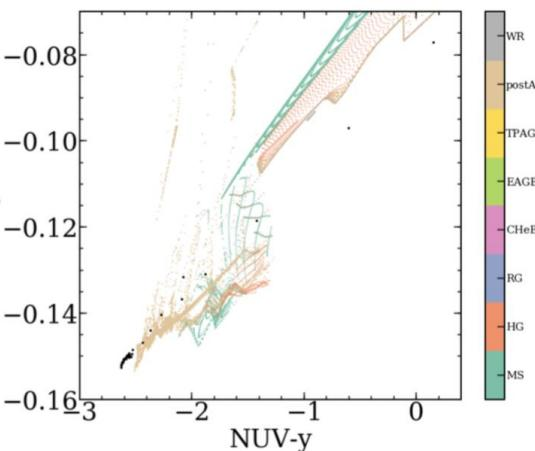
不同白矮星质量和吸积速率情况下，吸积白矮星的有效温度、半径和重力加速度



$$\log g = \log G + \log M - 2\log R$$

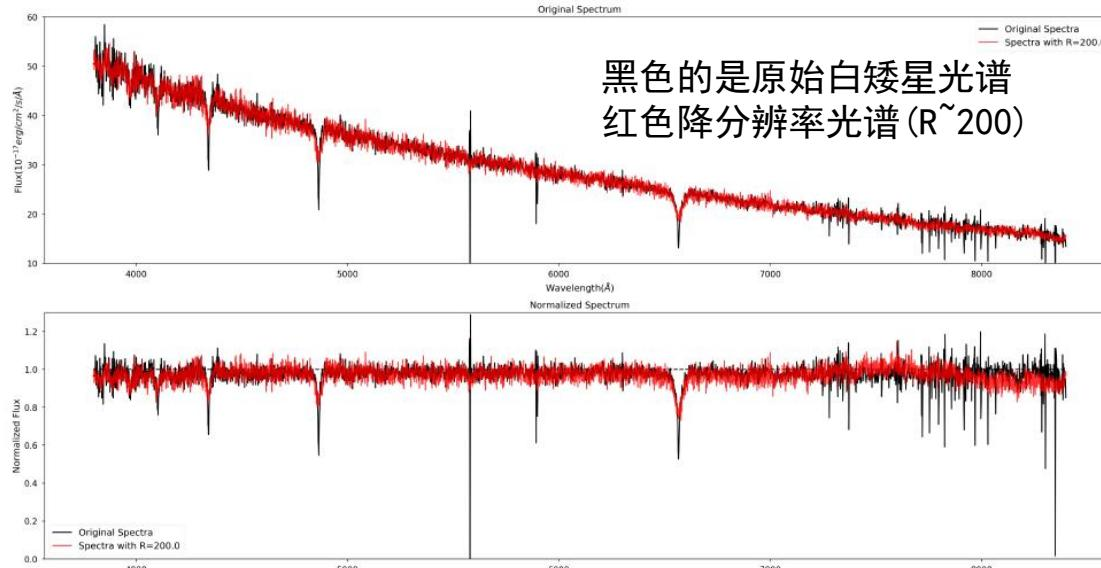


Xie+, 2022, RAA



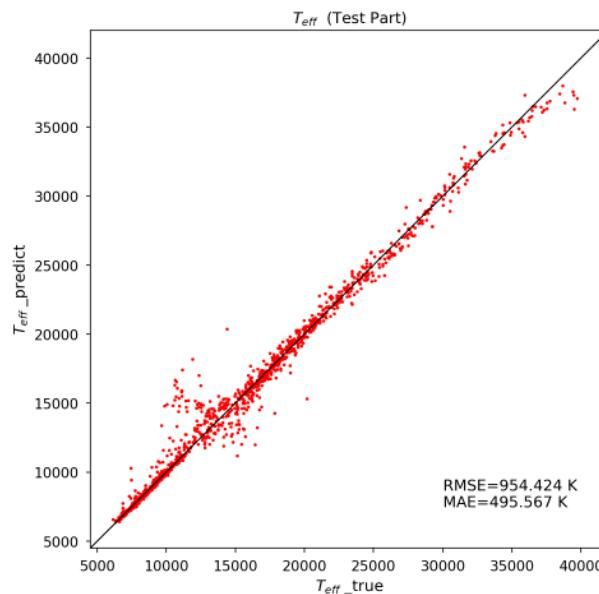
白矮星

绝大多数恒星最终都会演化成白矮星。



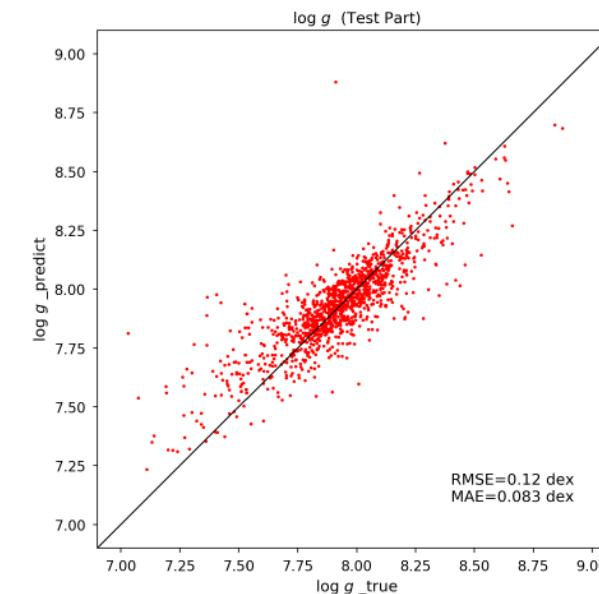
预测精度分别为
954K, 0.12dex

下一步，加入模拟噪音
估算视向速度精度



基于深度学习技术，建立了 $R \sim 200$ 的
DA白矮星光谱和有效温度、表面重力
的神经网络

赵景昆&任娟娟

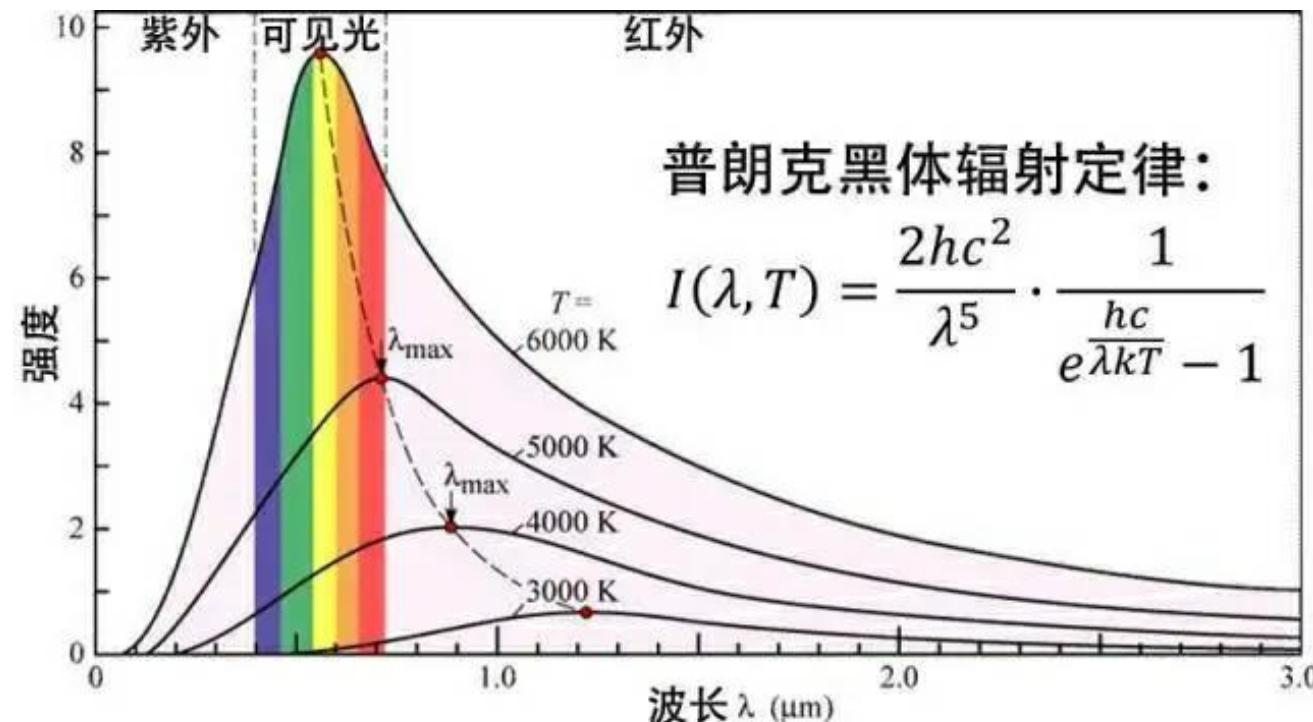


IV、红外流量法测量恒星有效温度 (Infrared Flux Method-IRFM)

通过比较恒星观测的热流量和红外单色流量之间的比值，与恒星表面热流量和红外单色流量之间的比值来确定恒星有效温度。

$$\frac{F_{\text{bol}}(\text{o})}{F_{\text{IR}}(\text{o})} = \frac{\sigma T_{\text{eff}}^4}{F_{\text{IR}}(\text{model})}$$

近红外的测光由连续谱主导，类似于瑞利-金斯的尾巴，几乎和有效温度线性相关。模型依赖的红外流量几乎不受金属丰度、表面重力加速度和米粒组织的影响。



The GALAH survey: effective temperature calibration from the InfraRed Flux Method in the Gaia system

Luca Casagrande^{1,2*}, Jane Lin^{1,2}, Adam D. Rains¹, Fan Liu³, Sven Buder^{1,2},

¹ Research School of Astronomy and Astrophysics, Mount Stromlo Observatory, The Australian National University, ACT 2611, Australia

² Department of Physics, University of Washington, Seattle, WA 98195, USA

³ Department of Physics, University of California, Berkeley, CA 94720, USA

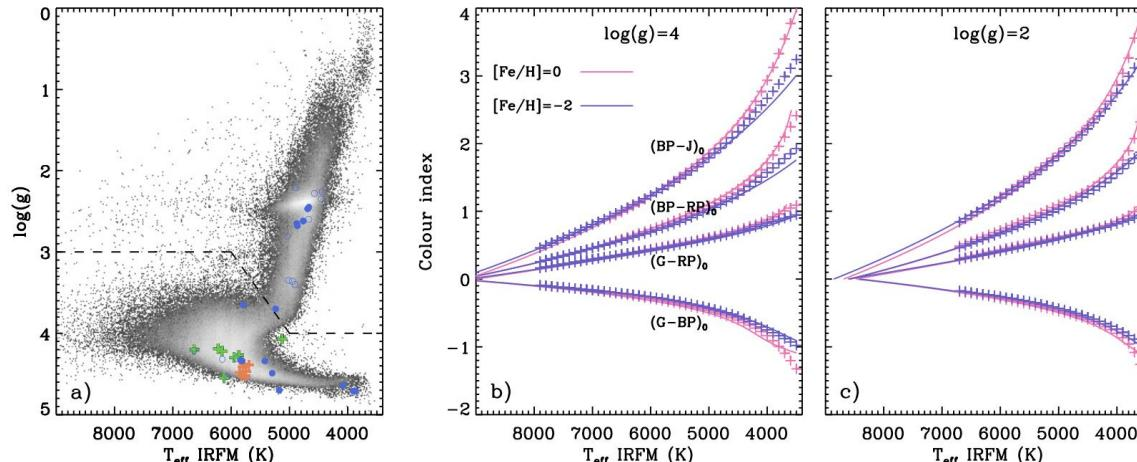
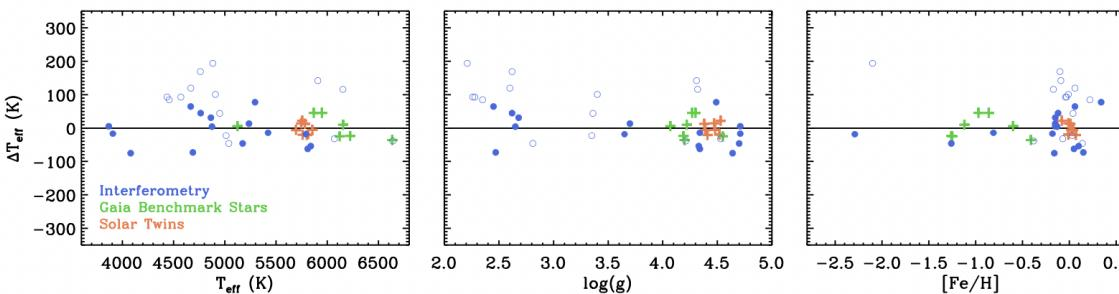


Figure 4. Panel a): Kiel diagram of the GALAH DR3 sample used to derive the colour- T_{eff} relations presented in this work. The dashed line marks the separation between dwarf and giant stars discussed in Section 4. Coloured crosses and circles are the stars used in Fig. 6 to test the T_{eff} scale. Panels b) and c):



we determine, be it from spectroscopy, or inferred by comparing against stellar models (e.g., Nissen & Gustafsson 2018; Choi et al. 2018).

While angular diameters measured from interferometry provide the most direct way to measure effective temperatures of stars

Among the many indirect methods to determine T_{eff} is the InfraRed Flux Method (hereafter IRFM), an almost model independent photometric technique originally devised to obtain angular diameters to a precision of a few per cent, and capable of competing against intensity interferometry in cases where a good flux

SkyMapper stellar parameters for Galactic Archaeology on a grand-scale

L. Casagrande^{1,2*}, C. Wolf¹, A. D. Mackey^{1,2}, T. Nordlander^{1,2}, D. Yong^{1,2} and M. Bessell¹

¹ Research School of Astronomy and Astrophysics, Mount Stromlo Observatory, The Australian National University, ACT 2611, Australia

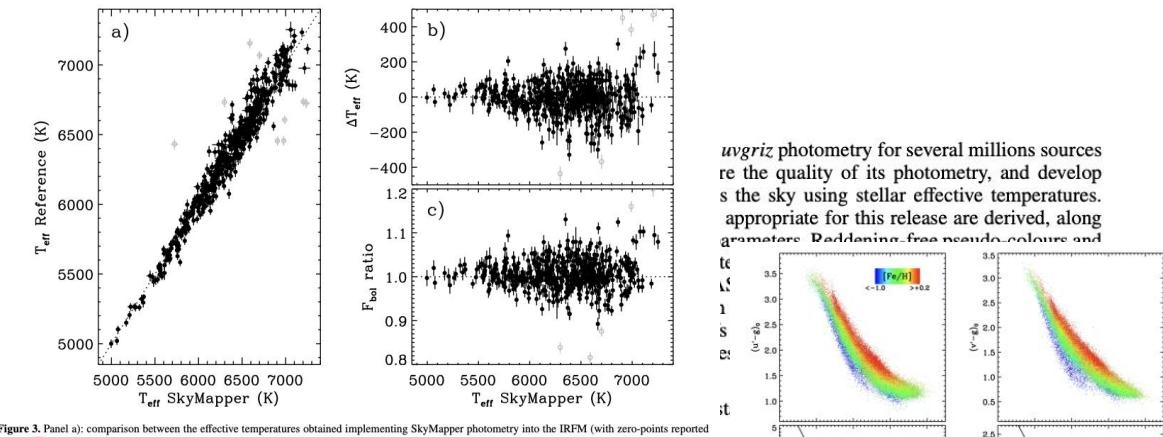


Figure 3. Panel a): comparison between the effective temperatures obtained implementing SkyMapper photometry into the IRFM (with zero-points reported

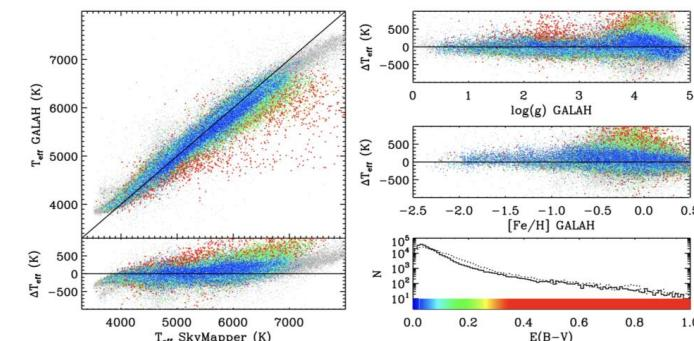
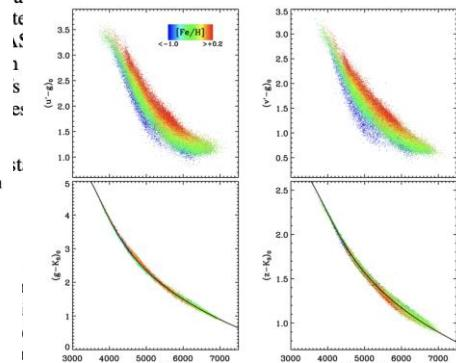


Figure 6. Comparison between T_{eff} derived implementing SkyMapper photometry into the IRFM, and the GALAH spectroscopic survey (Buder et al. 2018). Residuals (SkyMapper–GALAH) are shown as function of stellar parameters, and colour coded by reddening according to the scale in the bottom right panel. Dotted histogram is reddening from Schlegel et al. (1998), while continuous histogram shows the rescaled values we adopt. Grey points are stars flagged as unreliable in GALAH.

Wolf et al. (2018). The SkyMapper photometric system builds on the success of the $griz$ filters used by the Sloan Digital Sky Survey (Fukugita et al. 1996; Doi et al. 2010), with the added value of the uv bands, designed to be strongly sensitive to stellar parameters. The SkyMapper u band mimics the Strömgren u filter,

$uvgriz$ photometry for several millions sources re the quality of its photometry, and develops the sky using stellar effective temperatures. appropriate for this release are derived, along with reddening from pseudo-colours and

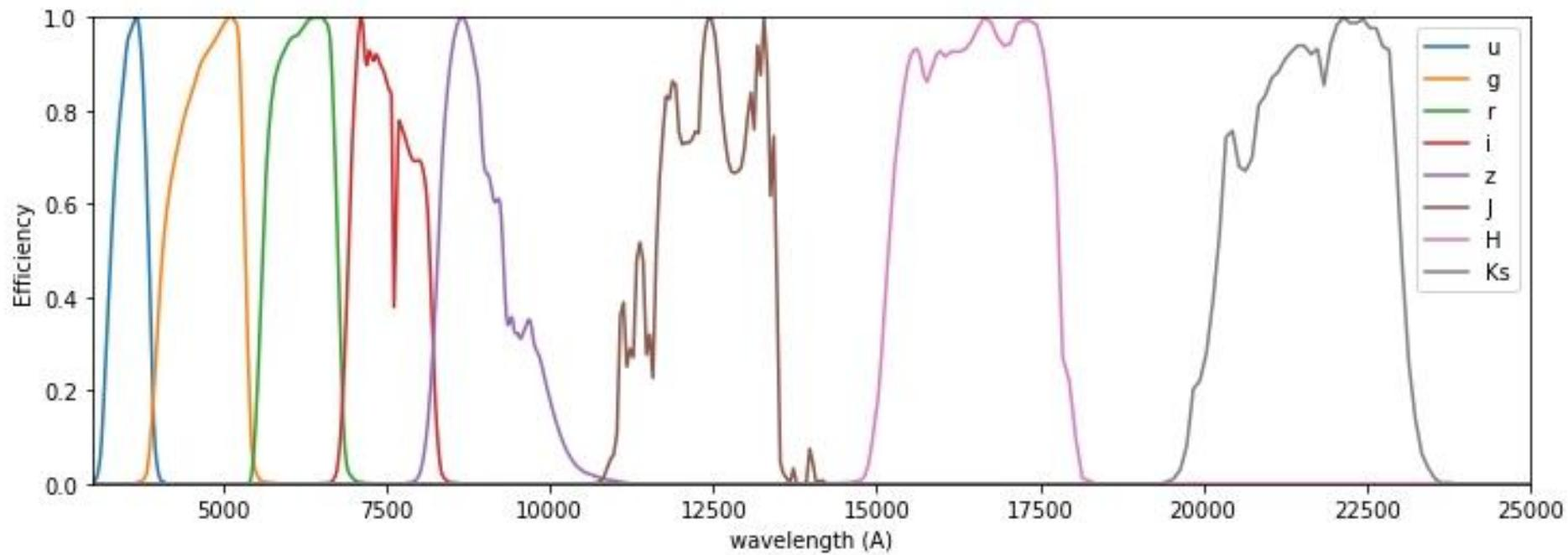


in the power of intermediate Strömgren uv photometric studies. Indeed, early SkyMapper data has already been successful at finding some of the most iron-poor stars (e.g., Keller et al. 2014; Howes et al. 2016). A full description of the SkyMapper photometric system can be found in I11.

SkyMapper made available its Data Release 1.1 (Buder et al. 2018), which provides $uvgriz$ magnitudes for over a billion objects across most of the southern sky although the goal of SkyMapper is to deliver mag-

system, when implementing a photometric system at the telescope it is not necessarily straightforward to adhere to the definition, and small zero-points offsets might be present. Knowledge of these offsets is important to assess the quality of the observations, to convert magnitudes into fluxes, as well as e.g., to compute theoretical synthetic colours to compare with observations.

Testing IRFM into SDSS



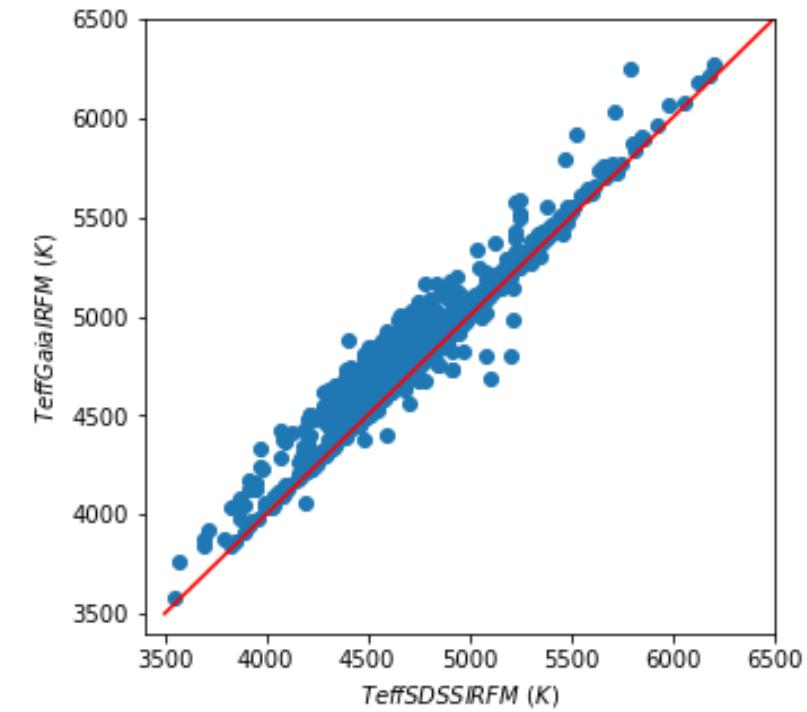
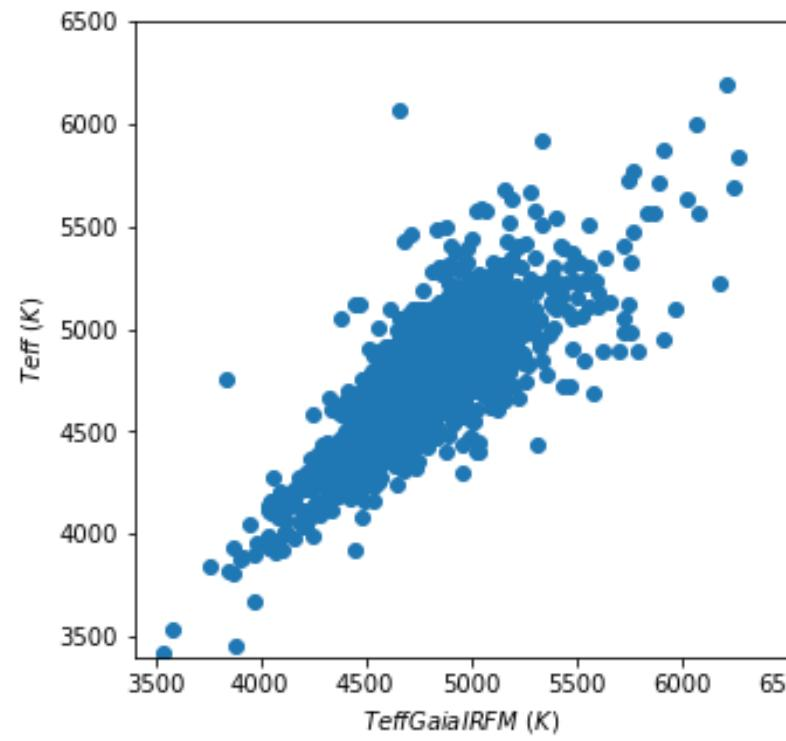
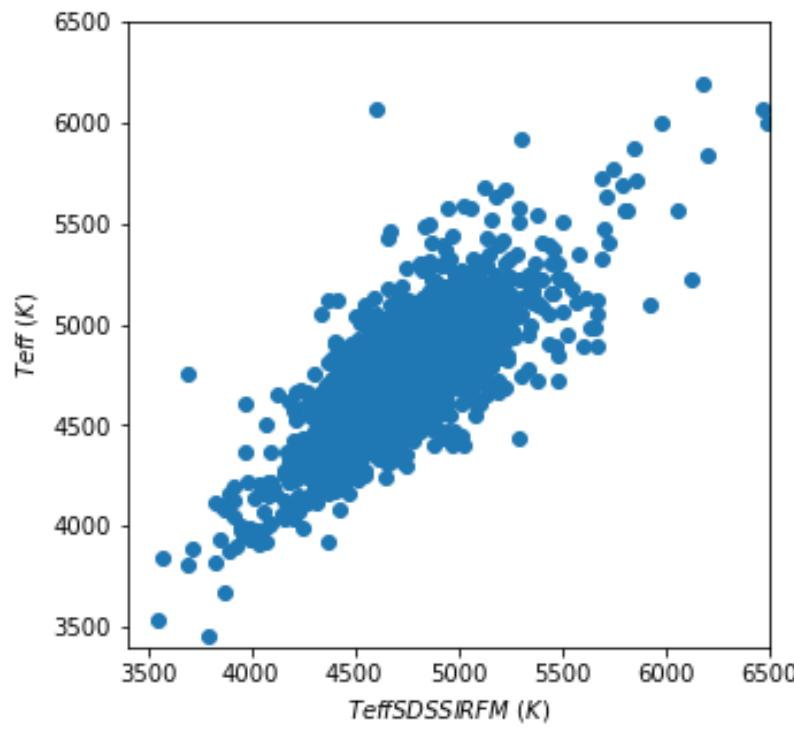
SDSS+2MASS各个波段系统通光效率

$$m_{\text{SDSS}} = m_{\text{AB}} + [0.04, 0., 0., 0., -0.02]$$

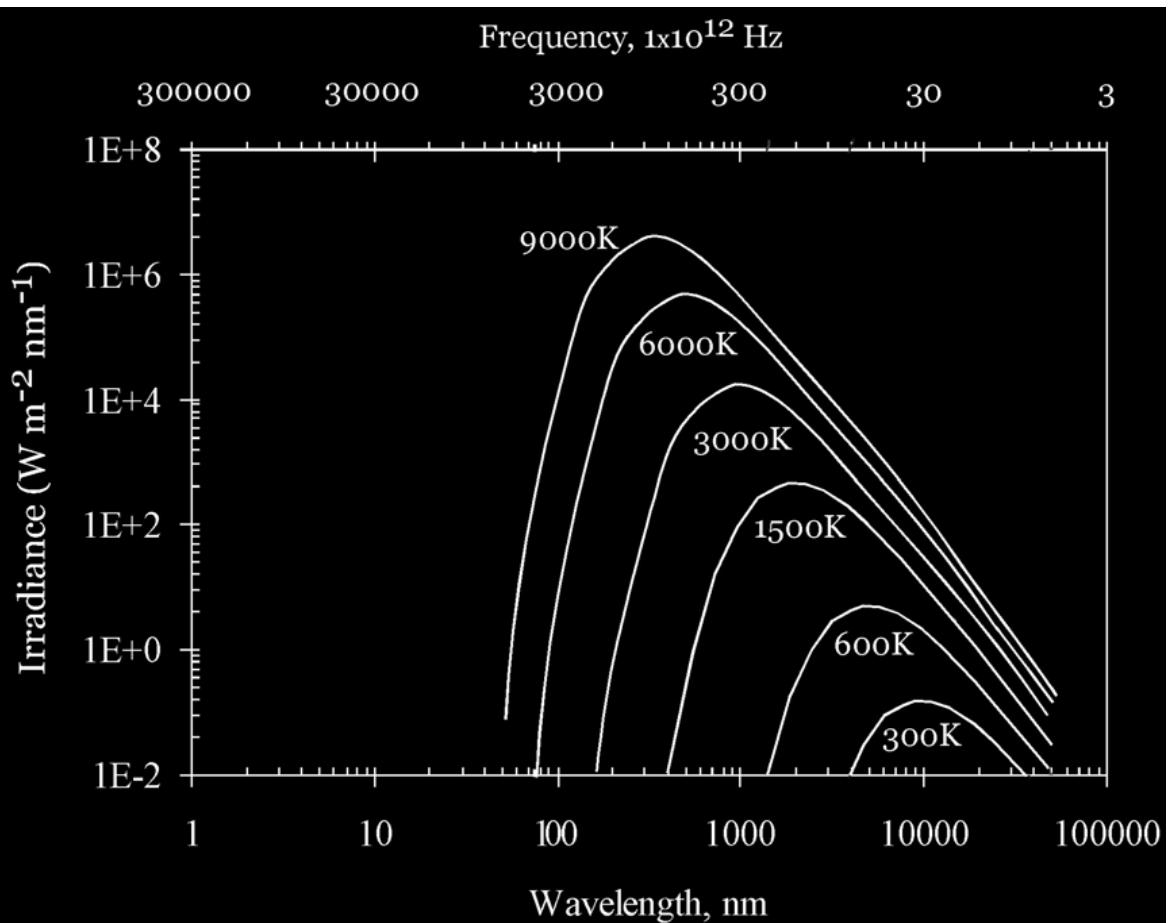
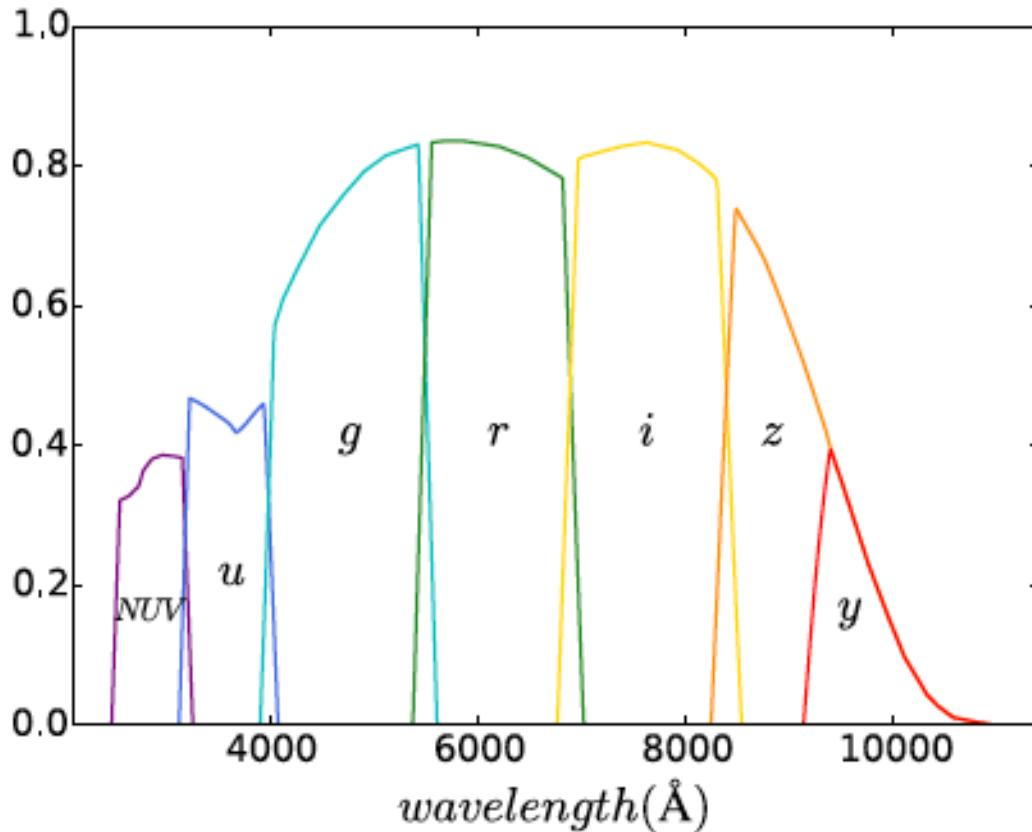
SDSS DR13 (1969颗)

Sloan photometry with errors less than 0.04 magnitudes,

2MASS with errors less than 0.05 mag



System response functions of CSST



OB stars and some hot white dwarfs
only CSST photometry will be suffice to derive Teff from the IRFM.

O 50,000 K
B0 25,000K
A0 11,000K

For later-type stars,

Euclid Y: 9200-11460

J: 11460-13720

H: 13720-20000

would provide necessary IR flux.

极限星等: 24 mag

V、基于LAMOST数据开展的双星研究

Searching SB2 using a binary spectral model

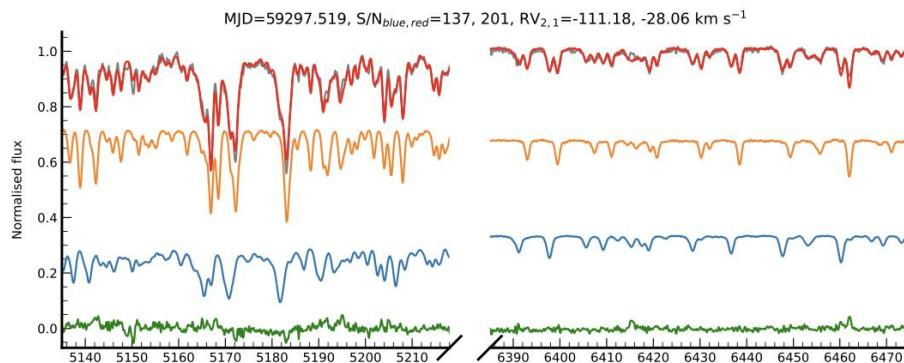
Kovalev+, 2022, MNRAS, 510, 1515;

MNRAS, 513, 4295;

MNRAS, in press (2460 SB2)

MNRAS, submitted

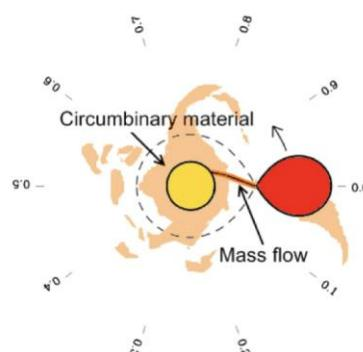
TYC 2990-127-1



处于物质交流阶段的红巨星+亚巨星

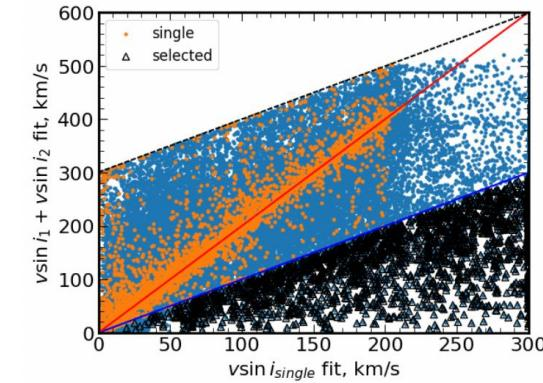
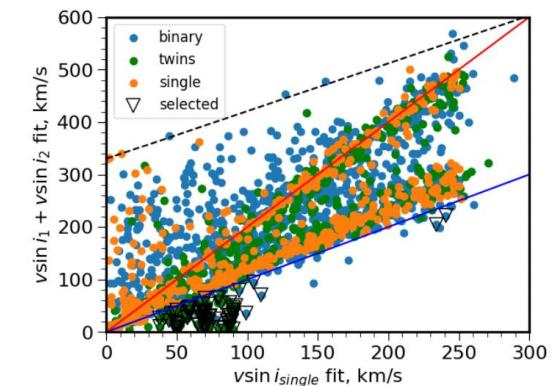
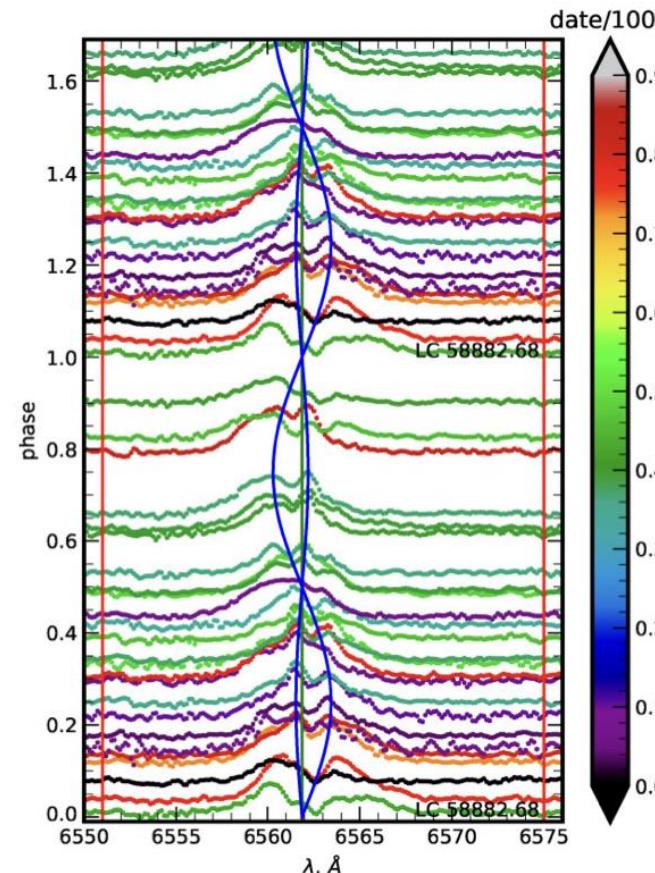
物质转移效率为30%

CSST ?



$$f_{\lambda, \text{binary}} = \frac{f_{\lambda,2} + k_{\lambda} f_{\lambda,1}}{1 + k_{\lambda}}, \quad k_{\lambda} = \frac{B_{\lambda}(T_{\text{eff},1}) M_1}{B_{\lambda}(T_{\text{eff},2}) M_2} 10^{\log(g)_2 - \log(g)_1}$$

$$f_{\text{imp}} = \frac{\sum \left[\left(|f_{\lambda, \text{single}} - f_{\lambda}| - |f_{\lambda, \text{binary}} - f_{\lambda}| \right) / \sigma_{\lambda} \right]}{\sum [|f_{\lambda, \text{single}} - f_{\lambda, \text{binary}}| / \sigma_{\lambda}]},$$



2460 SB2
1410 New

LAMOST-MRS

光谱双星的质量比 (LAMOST DR6 and DR 7) Li+, 2022, ApJ

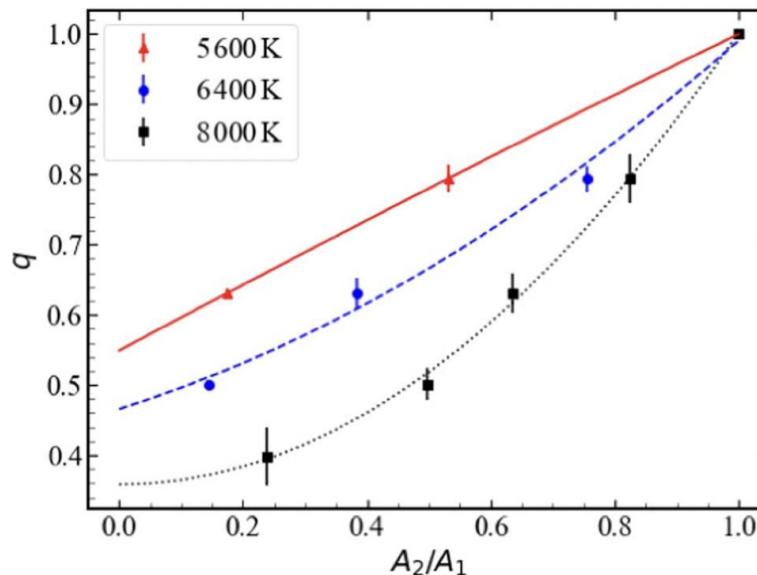
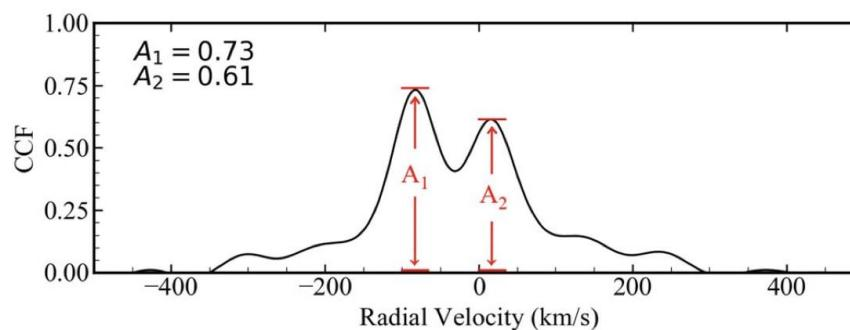
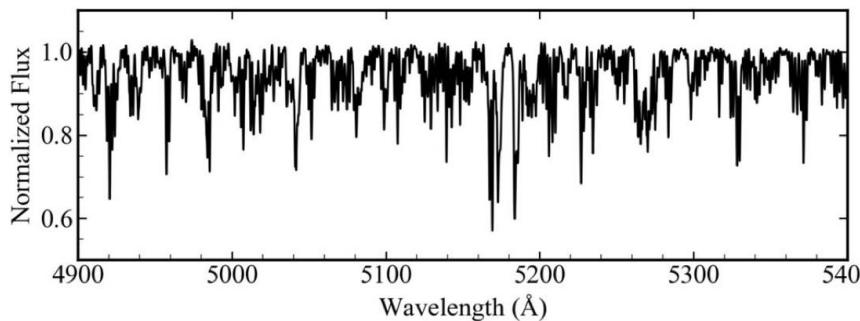
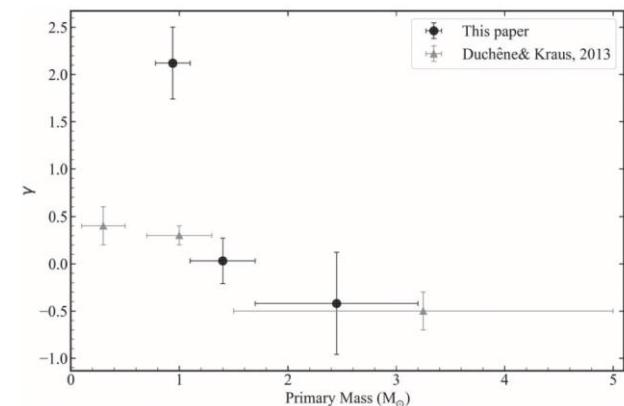
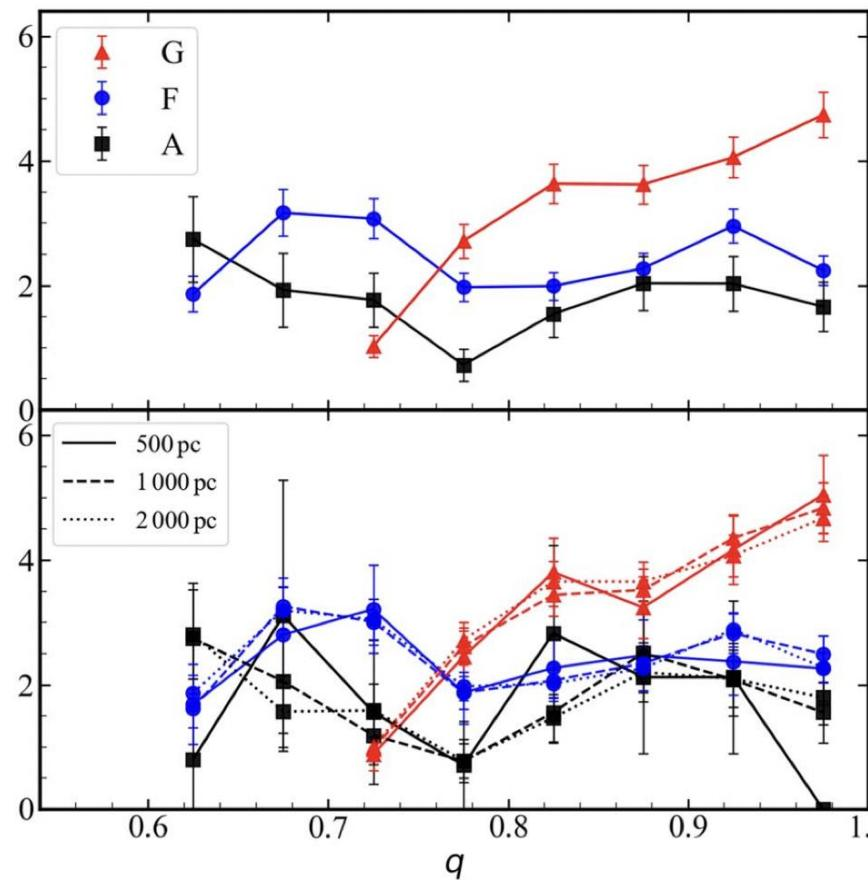


Table 1
The Number of SB2 Candidates Identified for Each Spectral Type (SPEC)

$T_{\text{eff}}(\text{K})$	SPEC	N_{ALL}	N_{SB2}	$N_{\text{SB2}}(500 \text{ pc})$	$N_{\text{SB2}}(1000 \text{ pc})$	$N_{\text{SB2}}(2000 \text{ pc})$
7200–8000	A	10,228	226	29	133	211
6000–7200	F	60,231	882	183	639	860
5150–6000	G	78,997	895	311	738	870
Total	All	149,456	2003	523	1510	1941

Note. N_{SB2} is the number of SB2 candidates from the LAMOST-MRS DR6 and DR7. The candidates are divided into three parts, i.e., spectral types, based upon their T_{eff} ranges. $N_{\text{SB2}}(500 \text{ pc})$, $N_{\text{SB2}}(1000 \text{ pc})$, and N_{SB2} (2000 pc) show the number of SB2 candidates within 500, 1000, and 2000 pc from the Sun, respectively.

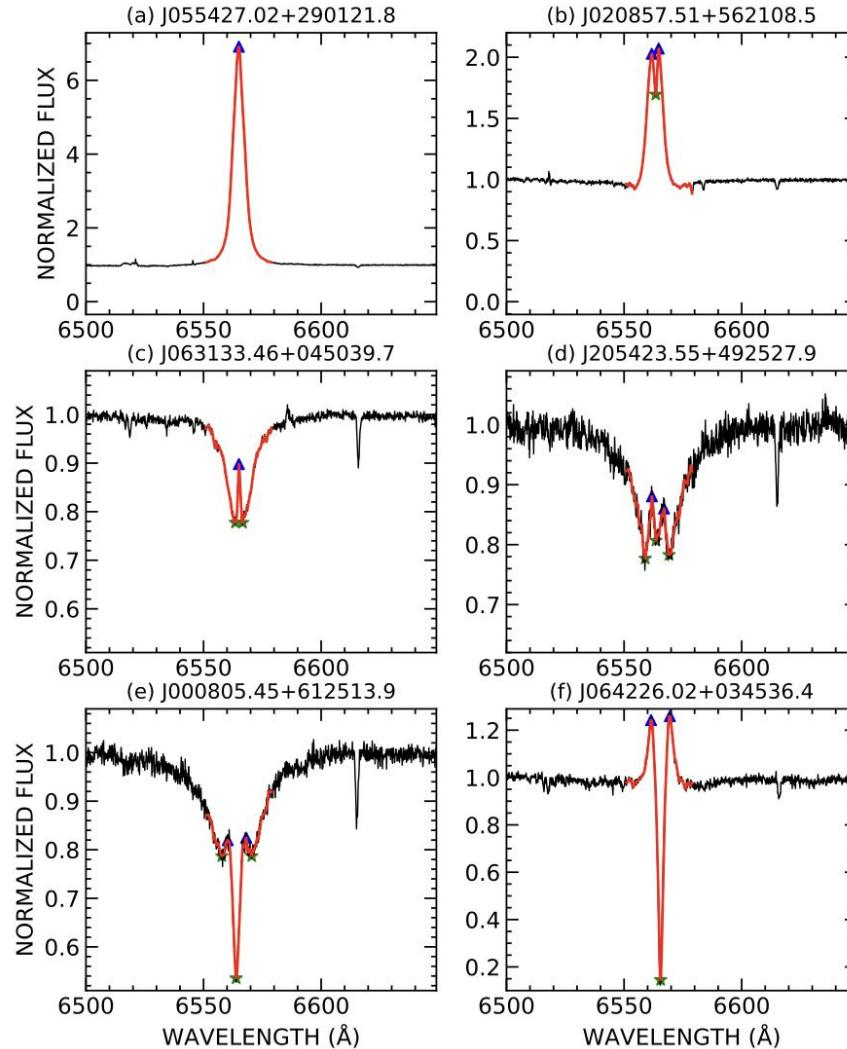


从LAMOST- MRS中寻找经典Be星 (to constrain massive binary evolution)

Wang+2022, ApJS, 260, 35

789,918 stars > 1162 candidates

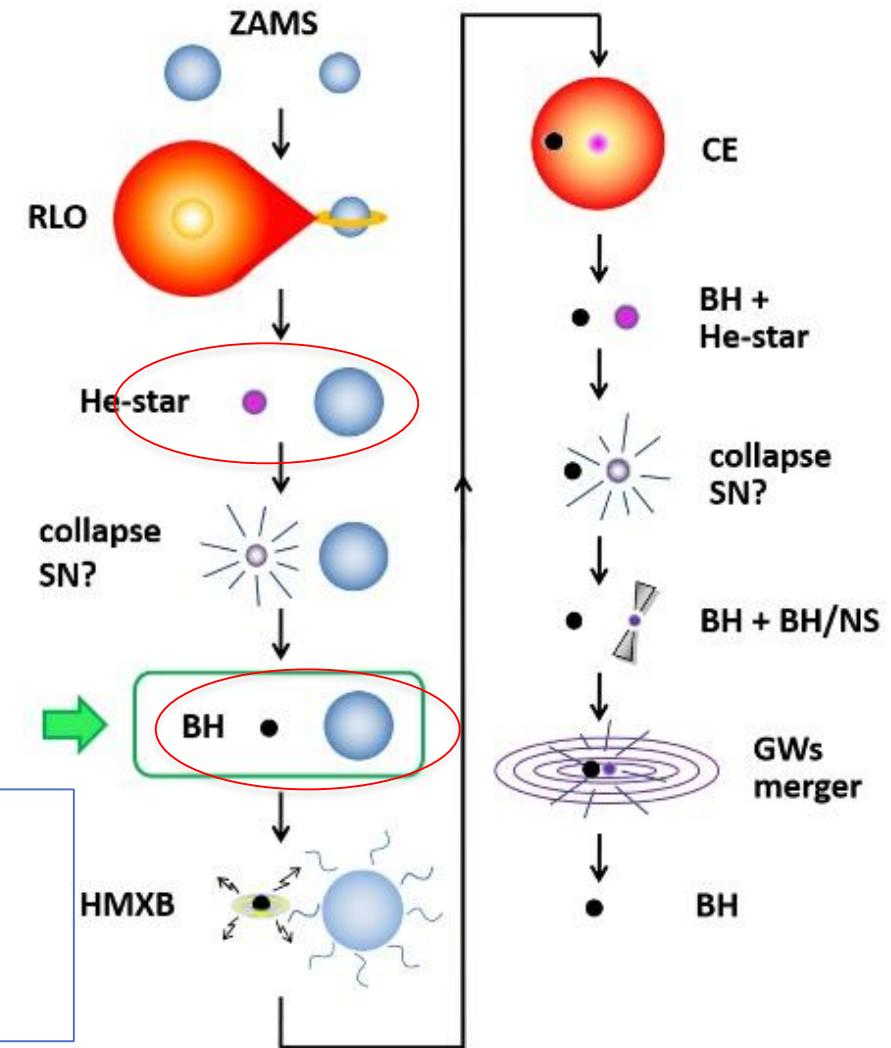
THE ASTROPHYSICAL JOURNAL SUPPLEMENT SERIES, 260:35 (20pp), 2022 June



151 known
183 new
41 in OCs
16 runaways



有很强的Balmar 发射线
~75% 碎裂速度
10,000-30,000K
2-20Msun



小 结

双星在天体物理的多个方面有重要作用。双星演化的基本问题长期未解决。作为双星星族合成模型的重要物理输入，双星比例和双星族的基本性质还存在较大争议。基于CSST的双星研究主要是探讨未来CSST在双星研究领域的潜力。

- 发展了一套多层神经感知模型来识别主序星双星； $SNR > 15$ 时，模型工作良好；
- 通过向前向量机器学习算法SLAM，基于CSST无缝光谱测量早型星的大气参数，误差小于10%。基于HST实测光谱测试显示误差在10%左右；
- 给出了基于CSST测光系统识别吸积白矮星的几组颜色-颜色图（观测误差未考虑）
- 正在发展基于CSST测光系统+Euclid的红外流量法测量恒星的有效温度；
- 基于LAMOST数据开展了一些算法和双星的搜寻工作，将尝试用于CSST。

谢谢！